

A SEARCH FOR SUBSTELLAR COMPANIONS TO SOLAR-TYPE STARS

BRUCE CAMPBELL¹

Department of Physics and Astronomy, University of Victoria; and Dominion Astrophysical Observatory,
 Herzberg Institute of Astrophysics

AND

G. A. H. WALKER¹ AND S. YANG¹

Department of Geophysics and Astronomy, University of British Columbia

Received 1987 December 14; accepted 1988 February 4

ABSTRACT

Relative radial velocities with a mean external error of 13 m s^{-1} rms have been obtained for 12 late-type dwarfs and four subgiants over the past six years. Two stars, χ^1 Ori A and γ Cep, show large (few $\times 10^3 \text{ m s}^{-1}$) velocity variations probably due to stellar companions. In contrast, the remaining 14 stars are virtually constant in velocity, showing no changes larger than $\sim 50 \text{ m s}^{-1}$. No obvious variations due to effects other than center-of-mass motion, including changes correlated with chromospheric activity, are observed.

Seven stars show small, but statistically significant, long-term trends in the relative velocities. These cannot be due to ~ 10 – 80 Jupiter mass brown dwarfs in orbits with $P \lesssim 50$ yr, since these would have been previously detected by conventional astrometry; companions of ~ 1 – 9 Jupiter masses are inferred. Since relatively massive brown dwarfs are rare or nonexistent, at least as companions to normal stars, these low-mass objects could represent the tip of the planetary mass spectrum. Observations are continuing to confirm these variations, and to determine periods.

Subject headings: planets: general — radial velocities — stars: binaries

I. INTRODUCTION

The nature and existence of objects less massive than the limit of the hydrogen-burning main sequence ($\sim 0.08 M_{\odot}$; D'Antona and Mazzitelli 1985) are important for a number of current astrophysical problems, including (a) determination of the minimum Jeans mass, (b) the mass limit for core hydrogen burning, (c) the cooling sequence for brown dwarfs, (d) identification of the "missing mass" component of the Galactic disk, and (e) the presence of massive halos around galaxies in general. At the extreme low end of the substellar mass spectrum are planets, which are distinct from brown dwarfs in that they probably form by solid-particle accretion in dissipated circumstellar disks, rather than by fragmentation and gravitational collapse of interstellar gas clouds (Black 1986). Detection of planetary companions to stars would answer a long-standing question in astronomy on the ubiquity of planetary systems, as well as help in understanding the formation processes of stars and planets.

The detection of substellar mass objects provides, however, a serious technological challenge. The low mass and luminosity of these objects makes the task of detecting them, let alone learning their physical characteristics, formidable. The most difficult problem is to detect extrasolar planets, and techniques for identifying objects of order a Jupiter mass ($\sim 0.001 M_{\odot}$), or smaller, have been reviewed by Bracewell and MacPhie (1979) and Black (1980). These techniques fall into the broad areas of direct detection by imaging or radar, and indirect detection by high-precision astrometry, radial velocities, or photometry. In all cases the expected signals are close to or below the limit of current detection capabilities.

We have developed a radial velocity technique which has sufficient precision to detect the reflex motion of stars due to orbiting substellar or planetary-mass objects. We have used this technique to monitor the relative velocities of 23 stars for the past six years. In this paper we will report on the results obtained to 1987 March for 16 of these stars. The precision of the relative velocities, and the time span of the observations, are now sufficient that we can make a preliminary assessment of the incidence of substellar mass companions to solar-type stars.

II. THE HYDROGEN FLUORIDE ABSORPTION CELL TECHNIQUE

a) Observational Procedures

This technique was first described by Campbell and Walker (1979). The principal feature of the technique is the introduction of an absorption cell containing hydrogen fluoride gas ahead of the slit of a coude spectrograph. Absorption lines of HF are superposed on starlight passing through the cell, as shown in Figure 1. The HF lines provide a wavelength calibration which is insensitive to optical or mechanical effects within the spectrograph. This is in contrast to the conventional technique, in which a *separate beam* of photons from a comparison source provides wavelength calibration. Instabilities and nonuniformities in the spectrograph components can lead to a relative displacement of the stellar and comparison spectra in the wavelength direction, which can result in relatively large systematic errors in radial velocities (Griffin and Griffin 1973).

Hydrogen fluoride was chosen for this application on the advice of Herzberg (1978). The R branch of the 3–0 vibration rotation band of HF is nearly ideal because (a) it produces strong absorption lines for a cell length of only 90 cm, (b) the lines are well spaced in wavelength, so that many stellar lines fall between, and (c) there is no interference by lines of rare

¹ Visiting Astronomer, Canada-France-Hawaii Telescope, operated by the National Research Council of Canada, the Centre National de la Recherche Scientifique of France, and the University of Hawaii.

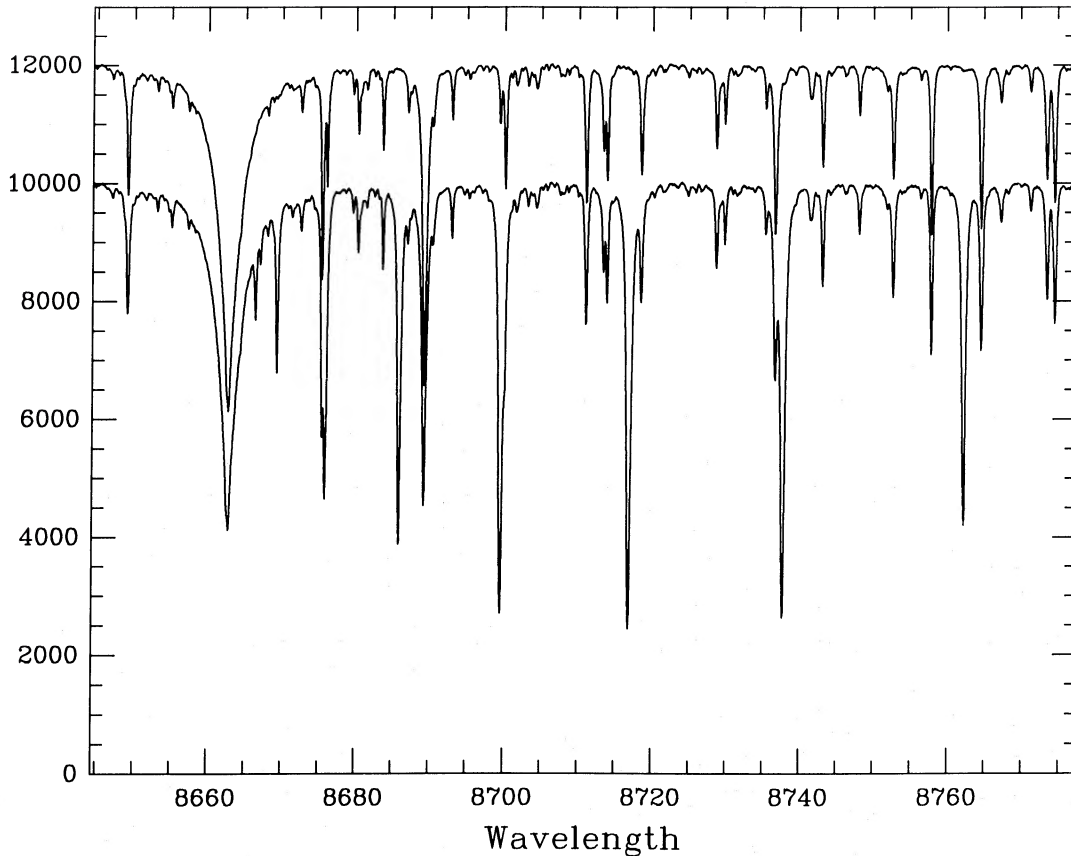


FIG. 1.—Spectra of 61 Cyg A with (*lower*) and without (*upper*) the R branch of the 3-0 band of hydrogen fluoride superposed

isotopes of HF, or by telluric absorption lines. To be sure, HF is a noxious gas, and so care in handling is required.

Stars were selected for observation if they were dwarfs or subgiants, were not known to be spectroscopic binaries, and had $\delta > -40^\circ$. A brightness limit of $I \lesssim 4.0$ was imposed, to ensure exposure times less than ~ 1 hr. Rapid rotators and stars earlier than type F5 were excluded, since such stars have too weak spectral lines for velocities of the highest precision.

We have been accumulating spectra of these stars since late 1980 with the f/8.2 coude spectrograph and HF cell of the Canada-France-Hawaii 3.6 m telescope. The detector is a Reticon photodiode array with 1872 elements (Walker, Johnson, and Yang 1985), which is photon-noise limited for the typical signal-to-noise ratio attained of about 1000. In such high-quality spectra the positions of strong absorption lines can be determined to about 0.01 pixels ($0.15 \mu\text{m}$), which, in the absence of systematic errors, results in a velocity precision of about 10 m s^{-1} for the ensemble of lines observed.

Changes in the wavelengths of the HF lines can occur with variations in temperature and pressure in the absorption cell. The slight run-to-run variations in these quantities ($\Delta T \lesssim 4^\circ\text{C}$; $\Delta P \lesssim 2$ torr) are adequately measured from the strengths of the hydrogen fluoride lines themselves, and corrections are made for wavelength shifts using the calibrations of Campbell and Walker (1979) and Campbell (1983). This procedure avoids depending on temperature and pressure meters, which could drift in gain or zero-point on a time scale of years.

For each stellar spectrum, the *mean* exposure time, which can differ significantly from the *mid*-exposure time, is derived

by integrating the output of the spectrograph flux meter. This step is essential in deriving accurate velocity corrections to the solar system barycenter, because the acceleration of the telescope by Earth rotation alone is about $2 \text{ m s}^{-1} \text{ minute}^{-1}$.

Following each stellar exposure, flat-field spectra are obtained with a special illumination system designed to precisely mimic the shape and collimation of the beam of starlight from the telescope. Experience has shown that such care is essential for accurate flat fielding.

b) Reduction to Relative Velocities

We give here only a brief summary of the reduction procedure, as the details have been described by Campbell *et al.* (1986). The reduction of these data was greatly facilitated by the spectrophotometric reduction package RETICENT (Pritchett, Mochnacki, and Yang 1982).

Each stellar spectrum with HF is first normalized relative to a reference stellar spectrum obtained without HF lines, and to a reference HF spectrum obtained with the flat-field lamp. This ensures that all instrumental effects are removed consistently from each stellar + HF spectrum. Line positions are then estimated after alternately cancelling either the stellar or HF lines by spectral division. Positions relative to those in the two reference spectra are derived using the difference technique of Fahlman and Glaspey (1973). Note that *relative* positions are of primary importance, since we are only looking for velocity *changes*. Approximate absolute line positions are only needed for registration of the spectra prior to spectral division.

The relative line positions so determined require correction

for two subtle effects. The first arises from convolution of the instrumental profile on blends of HF and stellar lines and has been discussed by Campbell and Walker (1985). Although this effect can introduce a slight random error in the velocities for individual stellar lines, it is not a problem in practice because severe blends are rejected, while adequate corrections can be derived for weaker blends. The second effect, discussed by Campbell *et al.* (1986), is more serious, since it can introduce a *systematic* error in the velocity from each spectrum. Changes in the asymmetry of the spectrograph instrumental profile can cause apparent displacements of spectral lines which are a function of line width. This is important since the hydrogen fluoride lines are on average about twice as wide as typical stellar lines. We correct this by measuring the instrumental asymmetry from HF lines, and by modeling the effect of the asymmetry variations on each line of each spectrum.

Relative velocities are determined from the corrected line positions by an iterative procedure, in which the HF line positions provide the zero point, while both the HF and the stellar lines provide the higher order terms of the dispersion relation. Weighted average velocities are then determined from, typically, 10–12 lines in each spectrum. The line weights are derived iteratively from the scatter of each line relative to the mean velocities in all spectra. This varying degree of scatter from line to line is partly an effect of line strength, but is probably also related to run-to-run changes in the high-frequency components of the dispersion relation (see Campbell *et al.* 1981). Finally, the mean velocity of each spectrum is corrected to the solar system barycenter using the routines of Stumpff (1980).

Table 1 summarizes the results for 16 program stars up to 1987 March. The first three columns show the times of observation (barycentric Julian date), the signal-to-noise ratios of the spectra (per continuum pixel), and the apparent relative velocities. The fourth column gives the relative velocities after correcting for run-to-run zero-point variations in the velocities. This is accomplished by using, for any given star, the velocities of all *other* stars (except χ^1 Ori A and γ Cep) observed in the same run to form a correction. In this step we make use of the fact that none of the program stars appears to show any significant short-term velocity variation, and so deviations about long-term trends can be used to determine the zero-point corrections. Observations with $|V|/\sigma_i > 3.0$ (see below) were not included in the corrections, and no correction was attempted if fewer than 4 independent observations were available. To illustrate their typical size, we show in Table 2 the corrections and their standard errors from all 14 stars for each of 27 observing runs. Observing runs were always three or fewer nights.

The fifth column of Table 1 shows the net internal errors, σ_i , for the corrected velocities. These internal errors are the quadrature sums of the standard errors from the velocities of all lines in each spectrum, and the standard errors in the run-to-run zero-point corrections. The corrected velocities with 1σ internal error bars are shown for each star in Figure 2.

III. ANALYSIS OF THE RELATIVE VELOCITIES

a) Tests for Velocity Variations

Before testing for possible long-term trends in the velocities, we first examined the velocities to check their error distribution. Figure 3 shows a histogram of the velocities divided by their internal errors for the 14 stars without large velocity

variations. (We take the ratio of the velocity to its internal error, since the scatter in the velocities is proportional to σ_i .) The curves in Figure 3 are from simulations of velocity data which mimic the actual data in the distribution of internal and external errors (see below). These curves show the anticipated distributions if no velocity trends are present, and if there is an average trend of $4\text{ m s}^{-1}\text{ yr}^{-1}$. The latter distribution matches reasonably well the actual data, except for seven velocities (from a total of 371) beyond 3.5σ . We ignore these velocities in the subsequent analysis, since these discrepant points could otherwise introduce spurious trends.

The remaining data for each star were fitted both with a straight line, and with a parabola, using a weighted least-squares procedure. Weights proportional to σ_i^{-2} were used. We have thus determined the first derivative (slope) and second derivative (curvature) of the velocities, and the formal 1σ uncertainties in each of these quantities. (Note that the slope and curvature are derived from *independent* fits to the data.) The slopes were corrected for secular acceleration (Campbell and Walker 1985), and, in two cases, for the predicted acceleration due to visual binary companions (cf. notes to ξ Boo A and 61 Cyg A below). Values of the corrected slopes, S , and curvatures, C , are given in Table 3.

The ratios of the absolute values of the slope and curvature to their respective errors ($|S|/\sigma_s$ and $|C|/\sigma_c$) are measures of the significance of long-term velocity variations. Figure 4 is a histogram of the observed $|S|/\sigma_s$ and $|C|/\sigma_c$, 28 values in total from the 14 stars. The continuous line in Figure 4 is the distribution derived from Monte Carlo simulations of 2000 sets of velocity data. Each such data set consisted of 27 velocities (the average number of observations per star) with the same time placement as the actual observing runs, while the rms deviation of the velocities at each point was just the actual scatter in the velocities for all stars observed in each of the 27 observing runs. Thus the simulated data accurately mimicked that for real stars on average, except that no velocity trends were imposed. Even though the rms deviations in velocity (external errors) are not the same from run-to-run, the simulated distributions of $|S|/\sigma_s$ and $|C|/\sigma_c$ are the same, and are normal distributions with $\sigma = 1$.

The observed distribution in Figure 4, when compared to that from the simulations, shows an excess above about 2.5σ . For seven stars $|S|/\sigma_s$ or $|C|/\sigma_c$ is greater than 2.5, whereas from the simulated distribution we would predict only 0.6 of 28 cases should be above this significance level, if no trends are present. We therefore believe that six of these seven stars have statistically significant variations in velocity. Since γ^2 Del has the lowest significance of this group (2.6σ), we conclude, somewhat arbitrarily, that its velocity variation is not significant. On the other hand, the variation for ϵ Eri is significant at the 4.1σ level, and so we classify this as a “probable” variable. For the other five stars in the 2.5 – 4.0σ range (36 UMa A, β Vir, 61 Vir, ξ Boo A, and β Aql A), the variations are small but statistically significant, and so we classify these as “possible” variables. The remaining eight stars we consider to be nonvariable within the errors of the present data set.

To test the effect of deleting velocities with $|V|/\sigma_i > 3.5$, we applied a 3.0σ rejection criterion, and repeated the analysis of the slopes and curvatures. An additional eight velocities were deleted in this case, but we found that removing these does not significantly alter our conclusions concerning velocity variations. Only γ^2 Del drops below the 2.5σ significance level.

The mean internal error, $\langle\sigma_i\rangle$, for each star is listed in

TABLE 1
RELATIVE RADIAL VELOCITIES

BJD 2440000+	Signal- to- noise	Relative velocity Apparent (m s ⁻¹)	Corrected (m s ⁻¹)	Internal error (m s ⁻¹)	Δ EW Ca II (mÅ)	BJD 2440000+	Signal- to- noise	Relative velocity Apparent (m s ⁻¹)	Corrected (m s ⁻¹)	Internal error (m s ⁻¹)	Δ EW Ca II (mÅ)
(a) HR 509 (τ Ceti)						(d) HR 1325 (α^2 Eridani A)					
4534.014	548	0.3	...	14.6	-3.2	4914.023	935	-18.8	-10.6	12.7	10.4
4621.742	348	42.9	18.5	24.6	-1.0	4926.932	1018	-29.9	-13.9	8.7	4.2
4653.739	670	26.3	-8.5	15.5	-0.9	4957.979	946	-0.2	-3.3	15.2	10.1
4654.723	925	23.8	-11.0	18.4	-0.1	5166.120	1008	-15.4	-19.4	11.8	-2.8
4771.134	973	-18.7	-29.3	13.0	1.2	5277.024	968	-3.3	-2.8	13.6	-6.8
4913.979	960	-20.9	-17.7	14.2	0.3	5357.714	947	25.2	...	10.2	-11.0
4926.855	1151	-4.1	12.0	12.0	0.4	5390.755	825	-49.6	-40.0	15.2	-4.2
4957.899	941	0.6	-4.1	13.7	-0.4	5711.835	1047	0.2	-1.8	13.6	8.6
5148.110	1134	-1.0	-13.6	8.8	-0.8	5712.888	1075	15.5	13.5	14.0	7.6
5166.083	968	6.0	5.0	9.6	-1.7	6047.918	1333	14.1	22.3	9.4	2.2
5213.043	854	-17.2	-20.0	5.7	1.4	6047.934	1545	15.5	23.7	11.2	2.9
5276.905	880	-16.9	-18.5	11.9	-1.1	6048.963	1598	5.3	13.5	12.5	1.4
5711.721	987	20.3	21.1	11.1	-1.6	6284.126	1044	7.7	21.8	19.0	-8.7
5712.799	609	32.0	32.8	12.6	-0.6	6284.139	1104	28.2	42.3	16.8	-9.1
5712.823	1044	-9.0	-8.2	10.4	-0.9	6393.943	1225	15.3	26.3	13.4	-1.5
5902.074	1286	-41.4	-25.4	11.2	1.1	6394.940	1281	10.0	21.0	11.1	-4.9
6047.809	1425	9.0	19.5	9.4	0.2	6725.984	1723	3.8	5.4	7.9	-3.6
6047.821	1314	7.5	18.0	8.3	-0.4	6726.939	1276	17.7	19.4	9.9	-4.4
6048.779	1159	17.4	27.9	9.2	1.8	6784.896	1409	12.5	11.6	15.4	4.1
6283.070	1067	-29.9	-20.0	13.0	1.5	6785.915	1638	1.1	0.2	11.9	-3.6
6283.083	899	-1.5	8.4	13.3	1.2	6834.835	1828	25.3	20.0	15.5	-1.4
6393.855	877	-8.8	-1.0	21.6	-1.4	6834.846	1387	18.3	13.0	10.7	-1.3
6393.863	1487	-23.2	-15.4	14.8	-1.2	6864.803	1535	-3.9	-12.4	14.5	-16.1
6394.876	1195	-17.1	-9.3	10.6	-0.3	6865.807	1433	-12.3	-20.8	12.6	-17.5
6604.127	929	-5.1	-1.9	8.6	0.8	6866.755	1440	-6.8	-15.3	6.6	-13.0
6605.119	1566	5.5	8.6	6.9	1.4	6866.762	1457	-14.5	-23.0	9.3	-12.8
6725.849	1120	1.4	0.9	7.6	1.0	(e) HR 2047 (χ^1 Orionis A)					
6725.858	1371	0.5	0.0	5.9	0.8	4958.034	879	1996.3	1642.8	18.8	11.6
6726.876	1521	1.0	0.5	6.7	0.0	5277.089	1050	2191.7	1842.8	14.9	-9.3
6784.844	1394	14.7	12.2	13.0	3.3	5357.797	815	2266.9	...	39.2	0.4
6785.866	1485	2.4	0.0	5.6	-0.5	5389.902	1001	2244.3	1904.1	21.0	4.6
6834.776	1625	10.6	1.4	8.5	0.4	5711.904	1003	2141.1	1790.9	10.0	-4.4
6864.731	1677	19.5	12.1	7.9	-0.3	5712.935	997	2098.3	1748.1	16.2	-5.4
6865.730	1523	3.6	-3.8	8.5	-0.1	5809.731	1083	1962.7	1625.8	11.8	-10.1
(b) HR 937 (ι Persei)						(c) HR 1084 (ϵ Eridani)					
4621.773	599	3.0	-44.2	23.1	0.1	4534.087	702	-9.7	...	19.7	15.6
4654.777	719	27.0	-7.6	19.9	0.7	4558.977	752	16.6	...	31.0	17.5
4655.739	858	38.4	3.8	22.4	2.3	4558.991	535	19.9	...	31.6	15.6
4914.001	859	-12.7	-7.9	17.2	1.3	4621.813	795	-7.6	-48.1	27.8	4.3
4926.883	1020	-23.1	-8.7	12.9	1.1	4653.843	779	-16.9	-51.5	19.3	4.5
4957.928	982	-9.6	-14.6	16.4	0.5	4655.768	794	5.8	-28.8	19.8	4.6
5149.115	235	-34.6	-45.7	26.1	3.0	4686.745	567	32.3	5.2	15.5	8.9
5276.938	915	33.9	35.7	16.0	-2.4	(d) HR 1325 (α^2 Eridani A)					
5711.760	992	22.9	24.7	12.4	0.2	4914.041	841	-7.9	-3.5	13.4	-4.9
5712.843	1046	18.4	20.1	11.1	0.1	4926.969	876	-18.2	-4.7	13.3	-1.4
6047.885	1492	-16.5	-10.7	6.3	-0.8	4958.000	1001	-1.0	-7.1	11.1	-3.2
6048.935	1535	-1.9	3.9	8.6	0.0	5277.047	899	35.7	34.5	11.8	-6.8
6284.040	732	18.4	31.8	20.2	-0.4	5357.749	1039	7.7	...	10.2	-2.8
6284.058	808	6.3	19.7	29.8	0.4	5711.868	1033	2.8	1.8	9.8	-7.1
6393.888	1353	8.1	18.4	16.4	-1.2	5712.905	1000	4.2	3.3	11.1	-6.5
6394.900	1028	-1.1	9.2	16.8	-1.2	6048.010	1248	-28.9	-23.4	8.1	-2.7
6725.927	1566	-11.6	-11.2	11.6	-1.0	6048.859	1367	-16.4	-10.9	7.2	-6.1
6726.901	1252	1.4	1.8	11.8	0.3	6393.959	1225	-16.4	-7.1	13.0	-1.9
6784.871	1366	-0.5	-2.6	8.4	1.5	6394.975	1269	16.6	25.9	11.8	-0.4
6785.954	1638	-6.0	-8.1	8.2	-2.0	6726.006	1332	6.1	5.2	12.0	2.8
6834.893	1689	12.6	4.7	12.1	-0.7	6726.954	1236	3.9	3.0	14.0	4.2
6864.830	1600	16.9	10.3	8.5	0.0	6784.922	1379	0.8	-3.7	8.1	10.6
6866.733	1816	2.8	-3.7	6.3	-1.6	6785.933	1550	-1.1	-5.6	5.7	5.8
(c) HR 1084 (ϵ Eridani)						(e) HR 2047 (χ^1 Orionis A)					
4534.087	702	-9.7	...	19.7	15.6	6834.866	1478	12.5	2.3	9.9	9.8
4558.977	752	16.6	...	31.0	17.5	6865.840	1433	18.7	11.2	9.4	6.5
4558.991	535	19.9	...	31.6	15.6	6866.793	1724	27.5	20.0	8.5	7.3
4621.813	795	-7.6	-48.1	27.8	4.3	(f) HR 1325 (α^2 Eridani A)					
4653.843	779	-16.9	-51.5	19.3	4.5	4559.032	534	-8.8	...	23.4	0.3
4655.768	794	5.8	-28.8	19.8	4.6	4653.887	557	34.5	-2.8	15.1	-1.3
4686.745	567	32.3	5.2	15.5	8.9	4655.818	876	26.2	-11.1	16.9	-1.8
(d) HR 1325 (α^2 Eridani A)						4686.771	442	89.2	56.0	40.2	-0.4
(e) HR 2047 (χ^1 Orionis A)						4914.041	841	-7.9	-3.5	13.4	-4.9
(f) HR 1325 (α^2 Eridani A)						4926.969	876	-18.2	-4.7	13.3	-1.4
(g) HR 2047 (χ^1 Orionis A)						4958.000	1001	-1.0	-7.1	11.1	-3.2
(h) HR 1325 (α^2 Eridani A)						5277.047	899	35.7	34.5	11.8	-6.8
(i) HR 2047 (χ^1 Orionis A)						5357.749	1039	7.7	...	10.2	-2.8
(j) HR 1325 (α^2 Eridani A)						5711.868	1033	2.8	1.8	9.8	-7.1
(k) HR 2047 (χ^1 Orionis A)						5712.905	1000	4.2	3.3	11.1	-6.5
(l) HR 1325 (α^2 Eridani A)						6048.010	1248	-28.9	-23.4	8.1	-2.7
(m) HR 2047 (χ^1 Orionis A)						6048.859	1367	-16.4	-10.9	7.2	-6.1
(n) HR 1325 (α^2 Eridani A)						6393.959	1225	-16.4	-7.1	13.0	-1.9
(o) HR 2047 (χ^1 Orionis A)						6394.975	1269	16.6	25.9	11.8	-0.4
(p) HR 1325 (α^2 Eridani A)						6726.006	1332	6.1	5.2	12.0	2.8
(q) HR 2047 (χ^1 Orionis A)						6726.954	1236	3.9	3.0	14.0	4.2
(r) HR 1325 (α^2 Eridani A)						6784.922	1379	0.8	-3.7	8.1	10.6
(s) HR 2047 (χ^1 Orionis A)						6785.933	1550	-1.1	-5.6	5.7	5.8
(t) HR 1325 (α^2 Eridani A)						6834.866	1478	12.5	2.3	9.9	9.8
(u) HR 2047 (χ^1 Orionis A)						6865.840	1433	18.7	11.2	9.4	6.5
(v) HR 1325 (α^2 Eridani A)						6866.793	1724	27.5	20.0	8.5	7.3
(w) HR 2047 (χ^1 Orionis A)						(x) HR 1325 (α^2 Eridani A)					
(y) HR 1325 (α^2 Eridani A)						4958.034	879	1996.3	1642.8	18.8	11.6
(z) HR 2047 (χ^1 Orionis A)						5277.089	1050	2191.7	1842.8	14.9	-9.3
(aa) HR 1325 (α^2 Eridani A)						5357.797	815	2266.9	...	39.2	0.4
(ab) HR 2047 (χ^1 Orionis A)						5389.902	1001	2244.3	1904.1	21.0	4.6
(ac) HR 1325 (α^2 Eridani A)						5711.904	1003	2141.1	1790.9	10.0	-4.4
(ad) HR 2047 (χ^1 Orionis A)						5712.935	997	2098.3	1748.1	16.2	-5.4
(ae) HR 1325 (α^2 Eridani A)						5809.731	1083	1962.7	1625.8	11.8	-10.1
(af) HR 2047 (χ^1 Orionis A)						5810.739	996	1990.8	1654.0	15.9	-8.2
(ag) HR 1325 (α^2 Eridani A)						6048.900	1511	1254.6	913.1	10.7	1.5
(ah) HR 2047 (χ^1 Orionis A)						6393.982	1034	-813.3	-1152.7	37.2	-1.4
(ai) HR 1325 (α^2 Eridani A)						6394.995	1399	-844.7	-1184.1	19.3	9.7
(aj) HR 2047 (χ^1 Orionis A)						6538.814	935	-1388.0	-1732.5	18.6	-3.8
(ak) HR 1325 (α^2 Eridani A)						6726.033	1424	-1555.4	-1904.1	9.0	-2.6
(al) HR 2047 (χ^1 Orionis A)						6727.008	1552	-1533.1	-1881.8	12.0	-2.3
(am) HR 1325 (α^2 Eridani A)						6727.024	1457	-1540.3	-1888.9	13.7	-1.9
(an) HR 2047 (χ^1 Orionis A)						6784.952	1343	-1477.2	-1828.1	15.5	7.4
(ao) HR 1325 (α^2 Eridani A)						6785.979	1440	-1508.2	-1859.1	10.1	-0.2

TABLE 1—Continued

BJD 2440000+	Signal- to- noise	Relative velocity		Internal error (m s ⁻¹)	$\Delta E W$ Ca II (mÅ)
		Apparent (m s ⁻¹)	Corrected (m s ⁻¹)		
6393.748	1170	-13.0	-6.3	13.1	-6.2
6394.769	1044	21.6	28.3	19.9	-6.5
6539.123	1495	-9.3	-8.9	8.6	6.5
6604.073	1279	-17.0	-17.3	8.9	-4.3
6633.954	1359	-19.6	3.0	10.7	-2.6
6725.776	1331	4.9	1.9	7.7	10.5
6726.803	1215	-1.0	-4.0	6.0	13.5
6784.785	1286	35.5	30.1	7.8	8.5
(p) HR 8974 (γ Cephei)					
4754.128	1223	924.3	708.3	13.7	2.7
4771.112	867	970.5	757.7	19.0	5.7
4957.884	960	806.8	596.0	12.2	0.6
5148.077	1176	691.4	474.8	8.8	-3.3
5166.048	964	679.4	470.9	9.6	-2.4
5212.958	553	633.9	436.9	13.7	-2.4
5276.884	927	610.1	404.0	10.8	-4.0
5711.703	1007	392.4	184.8	14.3	-2.5
5712.786	1098	372.0	164.4	11.2	0.4
5811.130	1355	313.5	119.3	10.1	-3.2
5865.136	1374	273.8	73.6	10.3	5.3
5902.042	1328	197.0	10.5	7.8	-1.3
6047.771	1740	119.5	-79.3	6.8	-1.4
6047.782	1799	102.0	-96.8	8.9	-1.3
6217.144	1302	-45.3	-252.1	13.3	13.6
6284.003	1196	-110.7	-305.0	20.0	-2.0
6284.009	1153	-108.3	-302.6	18.4	-2.3
6393.804	1229	-171.5	-368.2	16.0	-1.6
6394.858	1327	-154.1	-350.8	10.4	-2.5
6605.100	1319	-329.6	-532.3	5.4	-0.2
6725.830	1774	-425.1	-631.1	4.8	-1.5
6726.856	1301	-419.6	-625.6	6.7	-0.8
6784.821	1425	-486.2	-694.4	10.4	4.2
6785.843	1864	-495.1	-703.4	11.1	-0.1
6834.758	1872	-542.5	-757.5	8.9	-1.2
6865.700	1884	-535.7	-749.2	10.3	1.6

column (6) of Table 3. The external errors (σ_e) in column (7) are the weighted rms variations of the velocities for the nonvariables, or the rms deviations about the first- or second-order trends for the possible or probable variables. The average

TABLE 2

VELOCITY CORRECTIONS		
BJD 2,440,000+	ΔV_{corr} (m s ⁻¹)	σ_{mean} (m s ⁻¹)
4654.0	+37.1	2.3
4687.0	+35.4	6.9
4746.0	-4.7	4.6
4754.0	+11.8	5.9
4770.0	+8.6	7.4
4914.0	-3.6	3.1
4927.0	-12.7	4.0
4958.0	+6.6	3.1
5148.0	+12.4	4.6
5166.0	+4.4	4.8
5277.0	+2.0	3.2
5459.0	+11.5	5.0
5712.0	+3.3	4.5
5810.0	-10.1	1.6
5864.0	-4.1	3.1
5902.0	-17.7	5.0
6048.0	-5.4	2.8
6216.0	+2.6	2.8
6283.0	-9.9	4.7
6394.0	-7.5	2.9
6538.0	-2.4	5.0
6604.0	-1.5	2.0
6634.0	-23.3	1.8
6726.0	+1.7	1.5
6785.0	+4.0	1.5
6835.0	+10.8	2.9
6865.0	+9.3	2.1

external error for 14 stars (excluding γ Cep; see below) is 13 m s⁻¹, versus the average internal error of 10 m s⁻¹. The general agreement between the external and internal errors for all 14 stars implies that there are no obvious short-term velocity variations present in any of them. However, rapid variations could be present; a search for these will be the subject of a future publication. For the moment we note that these must have small amplitude, since the mean value of $(\sigma_e^2 - \langle \sigma_i^2 \rangle)^{1/2}$ is 8.0 m s⁻¹.

Two stars in the present sample show large velocity varia-

TABLE 3
SUMMARY OF RESULTS

HR (1)	Name (2)	Sp. (3)	S (m s ⁻¹ yr ⁻¹) (4)	C (m s ⁻¹ yr ⁻²) (5)	$\langle \sigma_i \rangle$ (m s ⁻¹) (6)	σ_e (m s ⁻¹) (7)	$r(V, \Delta EW)$ (8)	Companion mass ^a (M_{\odot}) (9)
509	τ Cet	G8V	+2.0 \pm 1.2	-2.6 \pm 1.7	9.4	13.9	-0.05	<4.2
937	ι Per	G0V	0.0 \pm 1.6	-2.6 \pm 1.8	11.3	13.7	-0.41	<13.3
1084	ϵ Eri	K2V	+2.3 \pm 1.7	-7.7 \pm 1.9	12.0	15.3	+0.02	1.2-4.7
1325	σ^2 Eri A	K1V	-1.1 \pm 1.6	+1.9 \pm 2.0	10.2	13.9	+0.06	<5.1
4112	36 UMa A	F8V	-4.7 \pm 1.6	+2.7 \pm 2.0	12.1	14.2	+0.67	1.2-14.7
4540	β Vir	F9V	-3.9 \pm 1.3	-0.4 \pm 1.5	10.7	12.9	-0.10	1.1-10.4
4983	β Com	G0V	-2.3 \pm 1.4	-3.3 \pm 1.7	11.4	14.0	+0.33	<9.6
5019	61 Vir	G6V	-0.6 \pm 1.7	+5.2 \pm 1.8	10.2	13.3	-0.05	0.9-7.4
5544	ξ Boo A	G8V	-7.3 ^b \pm 1.9	-4.3 ^b \pm 1.5	11.3	13.6	+0.04	1.6-7.5
7462	σ Dra	K0V	-1.2 \pm 1.4	+2.8 \pm 1.6	10.0	10.1	-0.25	<6.1
7602	β Aql A	G8IV	+3.9 \pm 1.2	+0.8 \pm 1.8	8.3	10.7	-0.17	1.1-14.3
7948	γ^2 Del	K1IV	+3.2 \pm 1.4	+5.1 \pm 2.0	8.5	13.3	+0.40	<60.
7957	η Cep	K0IV	-0.6 \pm 1.6	+1.0 \pm 2.1	9.5	13.9	-0.09	<16.3
8085	61 Cyg A	K5V	+0.4 ^b \pm 1.9	+1.5 \pm 2.7	10.2	14.7	+0.01	<3.4
8974	γ Cep	K1III-IV	-263.2 \pm 4.8	-28.3 \pm 2.9	9.3	18.4 ^c	-0.02	1.7

^a Lower limits and value for γ Cep are $M_c \sin i$, upper limits are $M_c \sin^{1/3} i$.

^b Corrected for the effects of the visual binary companion.

^c Rms variation of velocity residuals about second order fit.

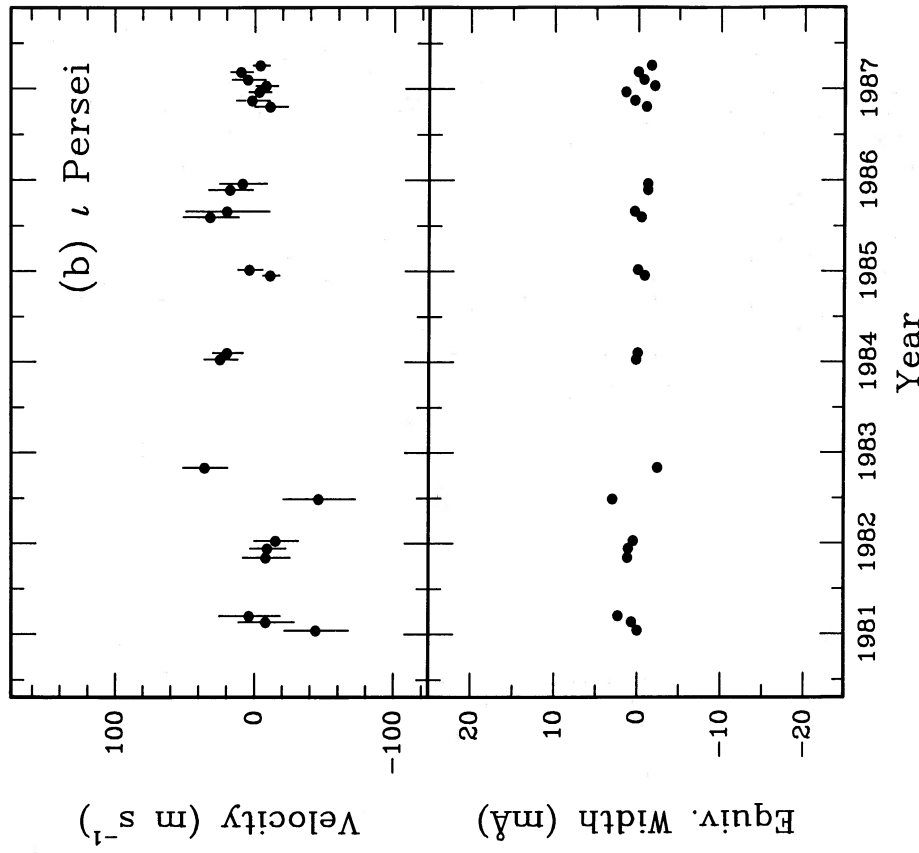


FIG. 2b

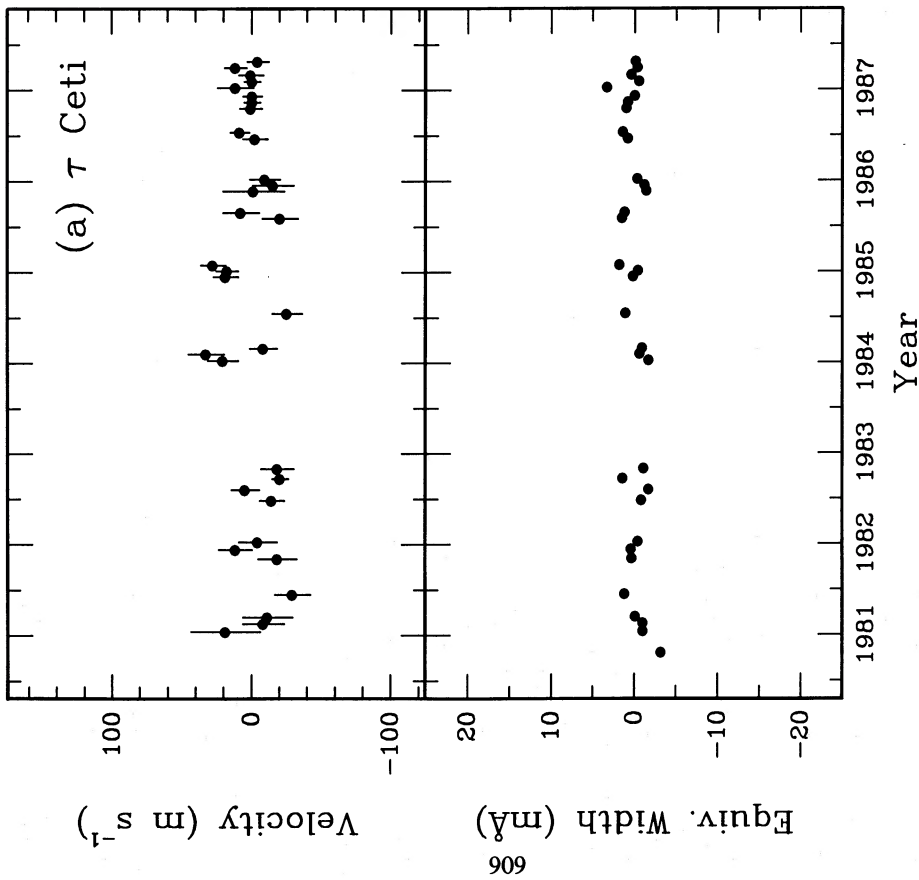


FIG. 2a

FIG. 2.—(a-p) Relative velocities (*upper panels*) and Ca II $\lambda 8662$ equivalent widths (*lower panels*) for 16 stars. Velocity and equivalent width scales have arbitrary zero points. Error bars on velocities are 1σ internal errors. For clarity, some points have been shifted horizontally to avoid overlap.

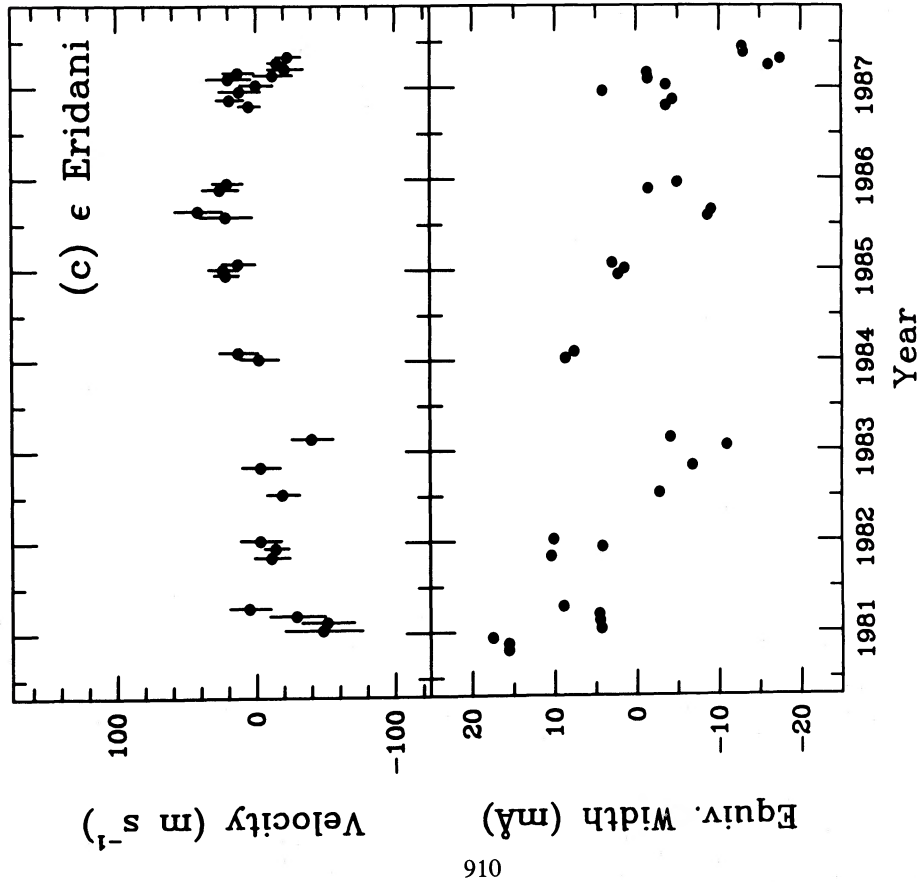


FIG. 2c

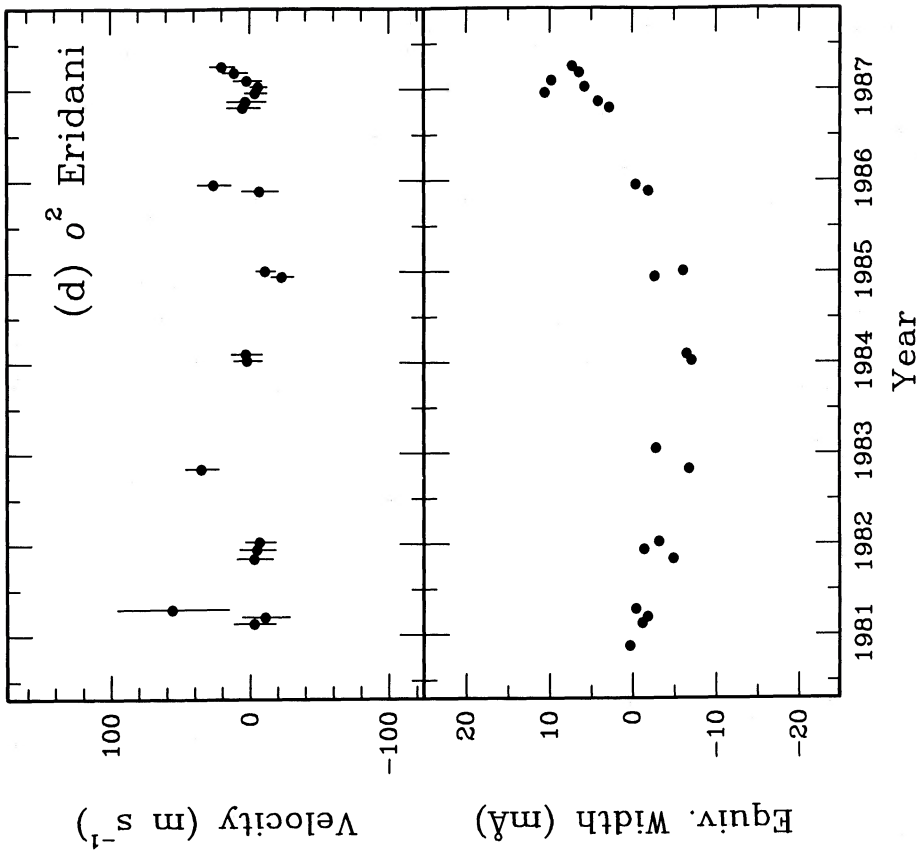


FIG. 2d

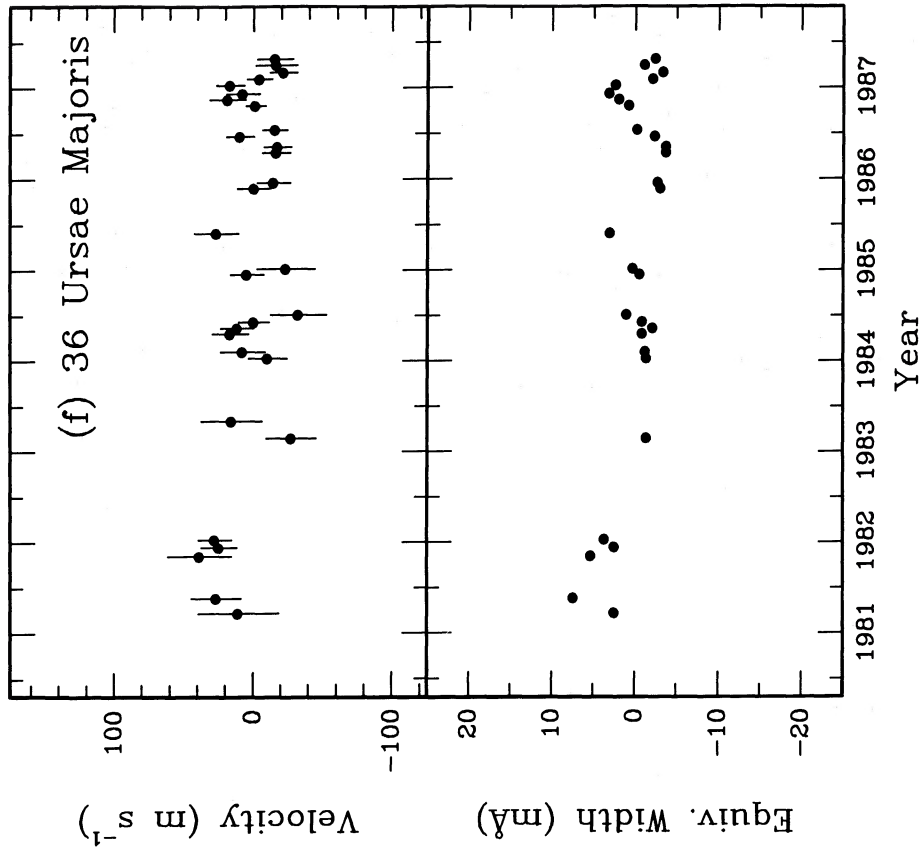


FIG. 2f

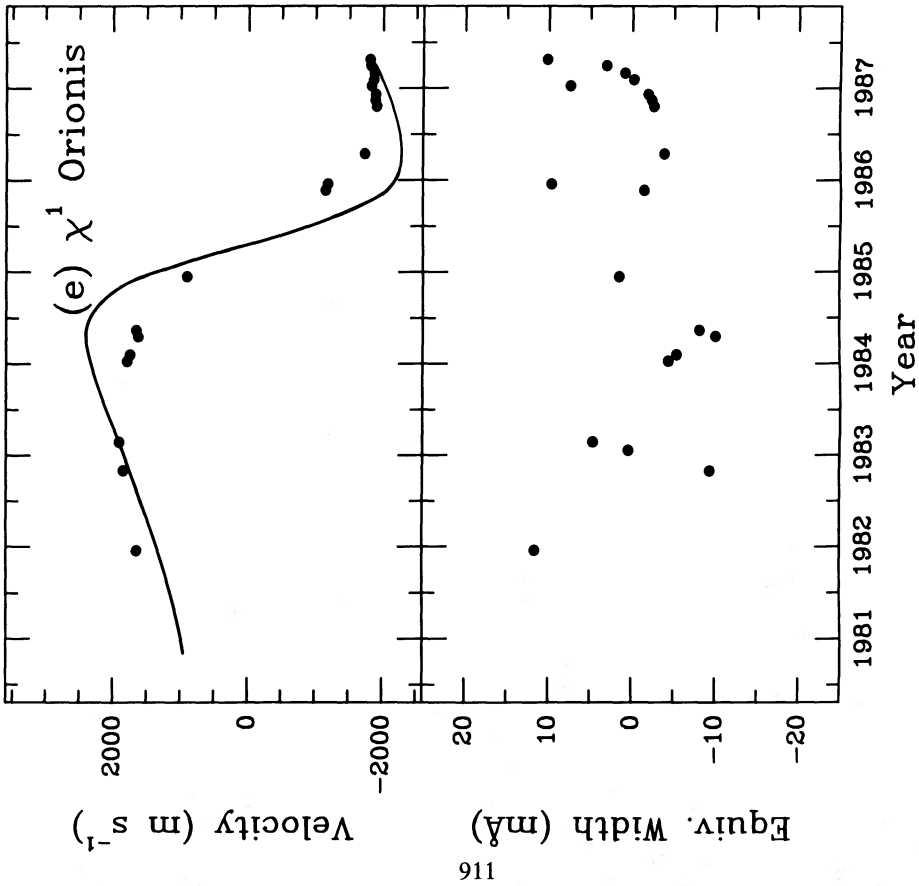


FIG. 2e

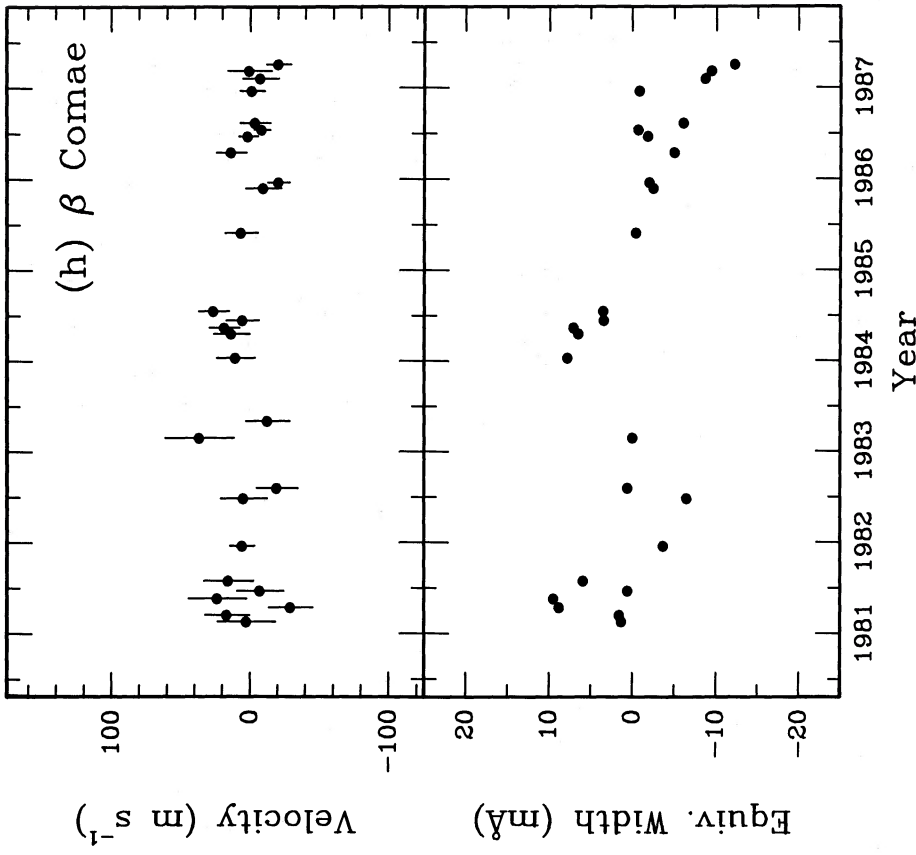


FIG. 2h

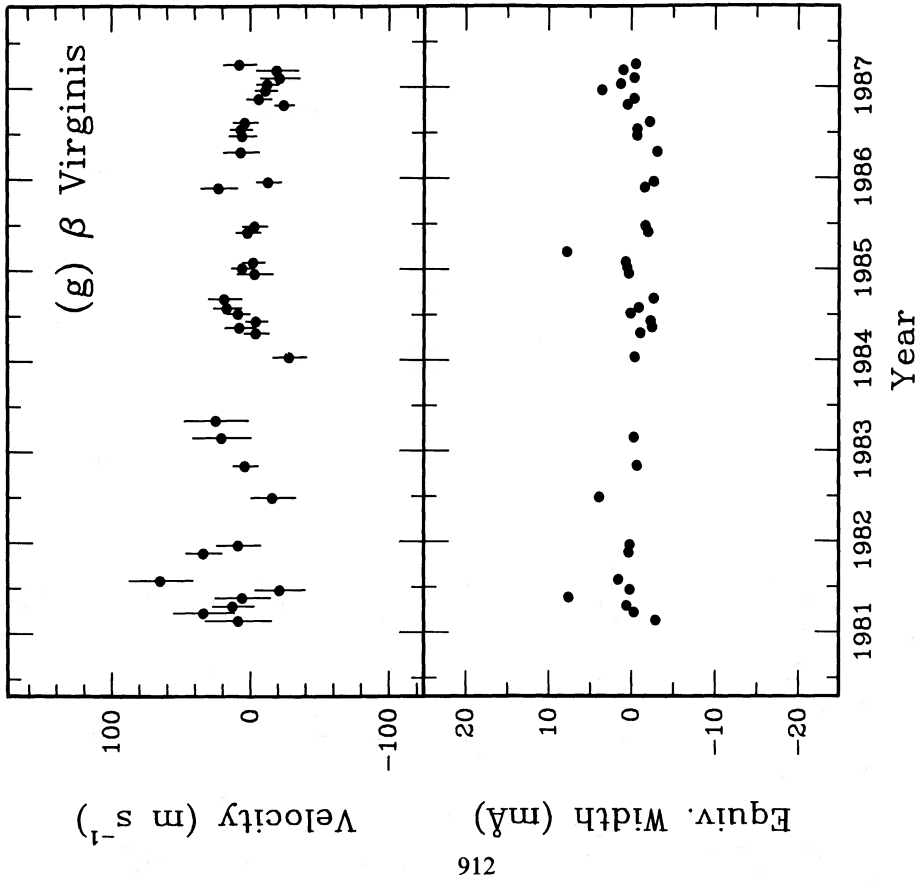


FIG. 2g

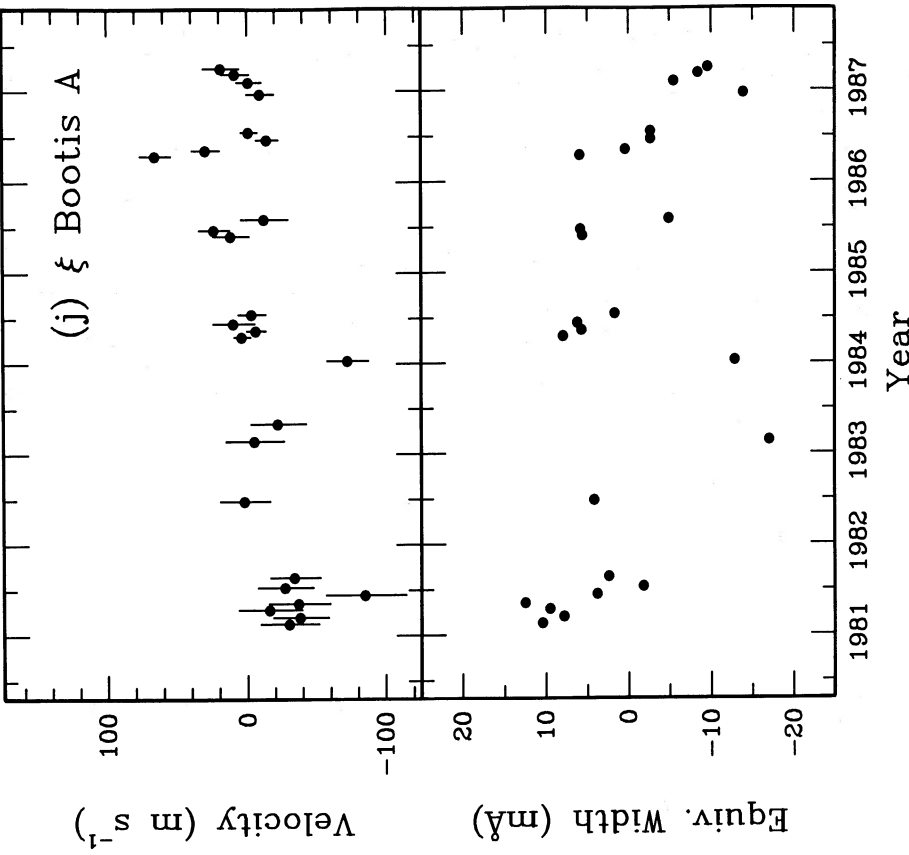


FIG. 2j

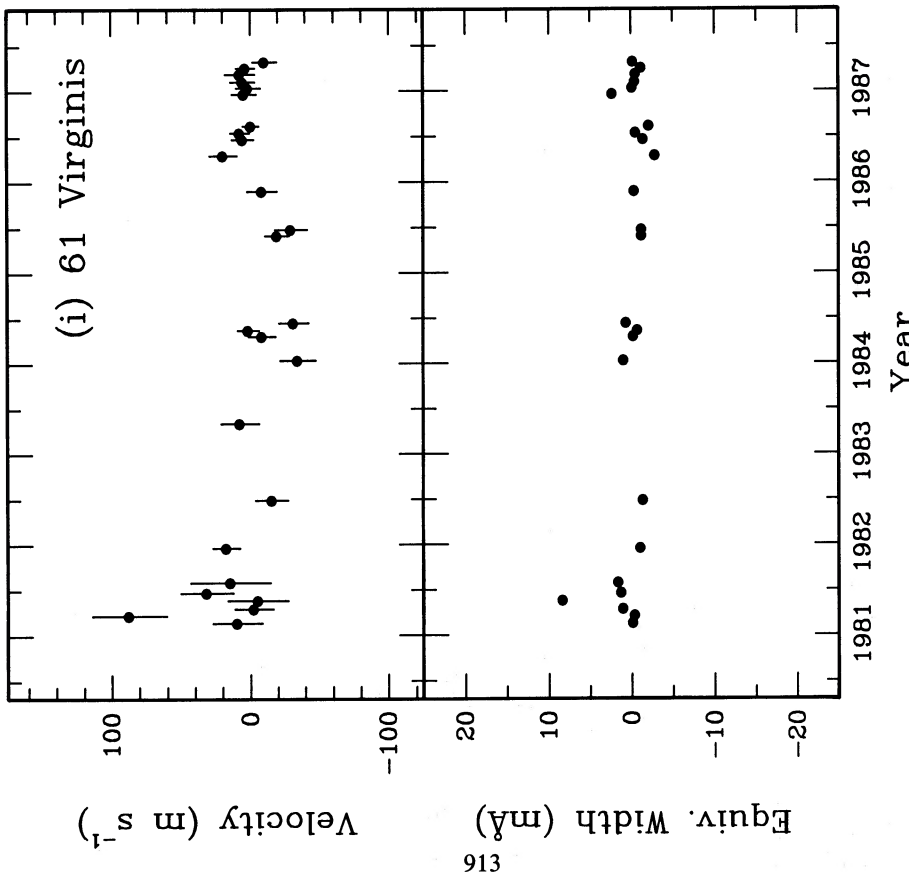


FIG. 2i

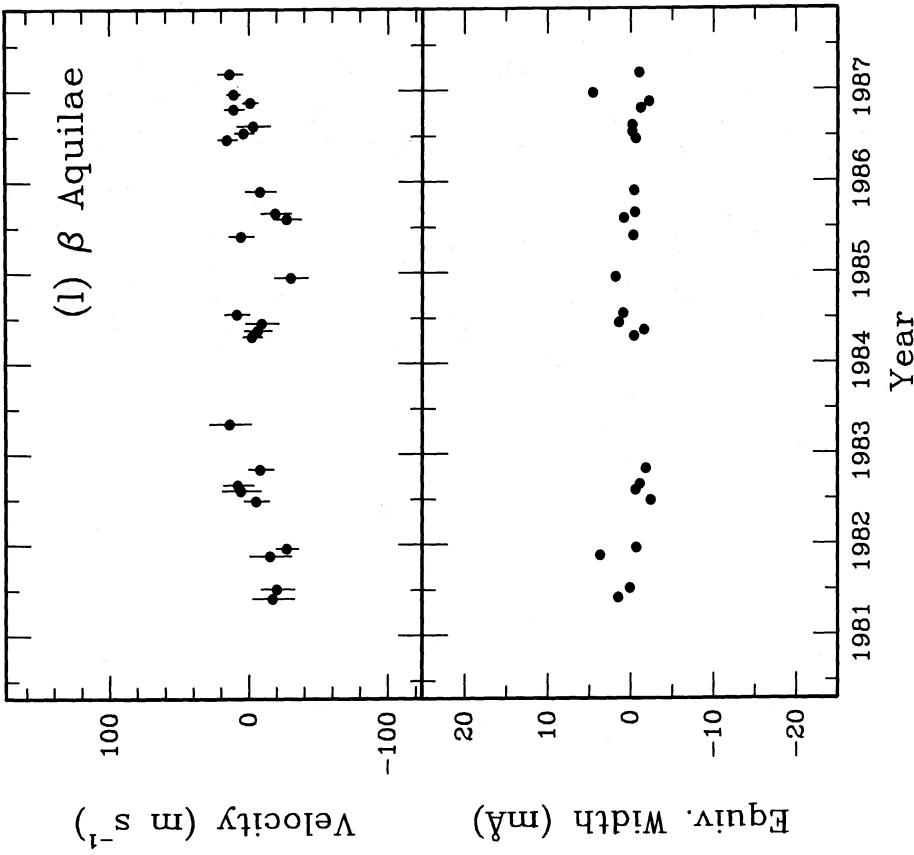


FIG. 2l

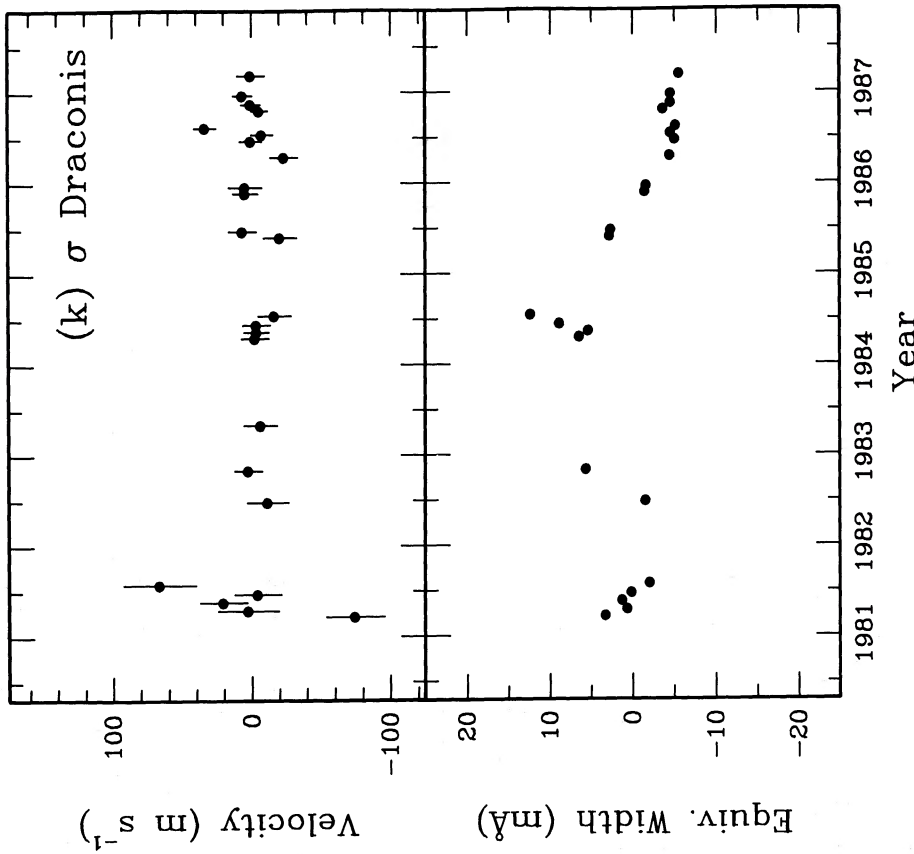


FIG. 2k

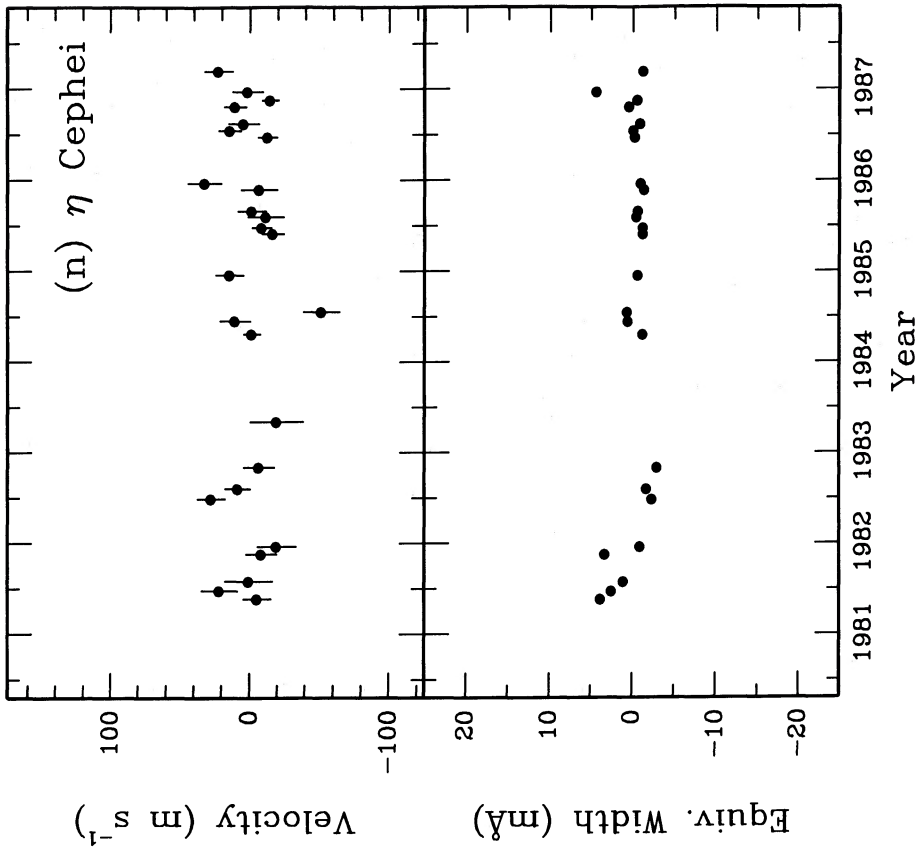


FIG. 2n

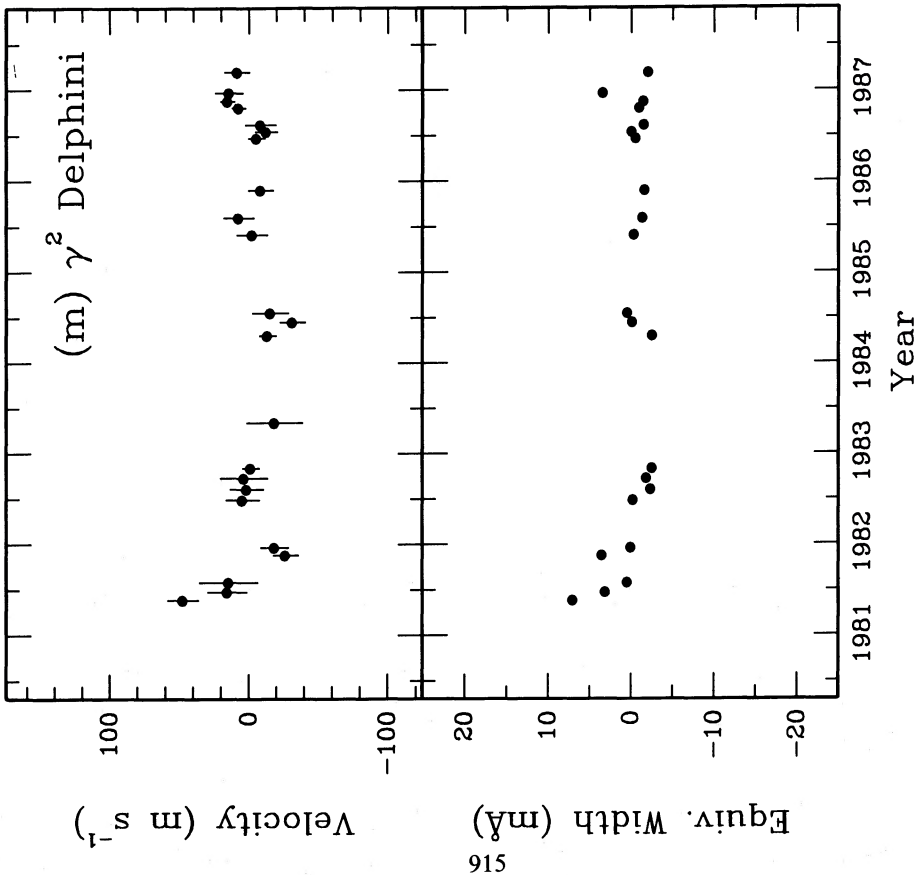


FIG. 2m

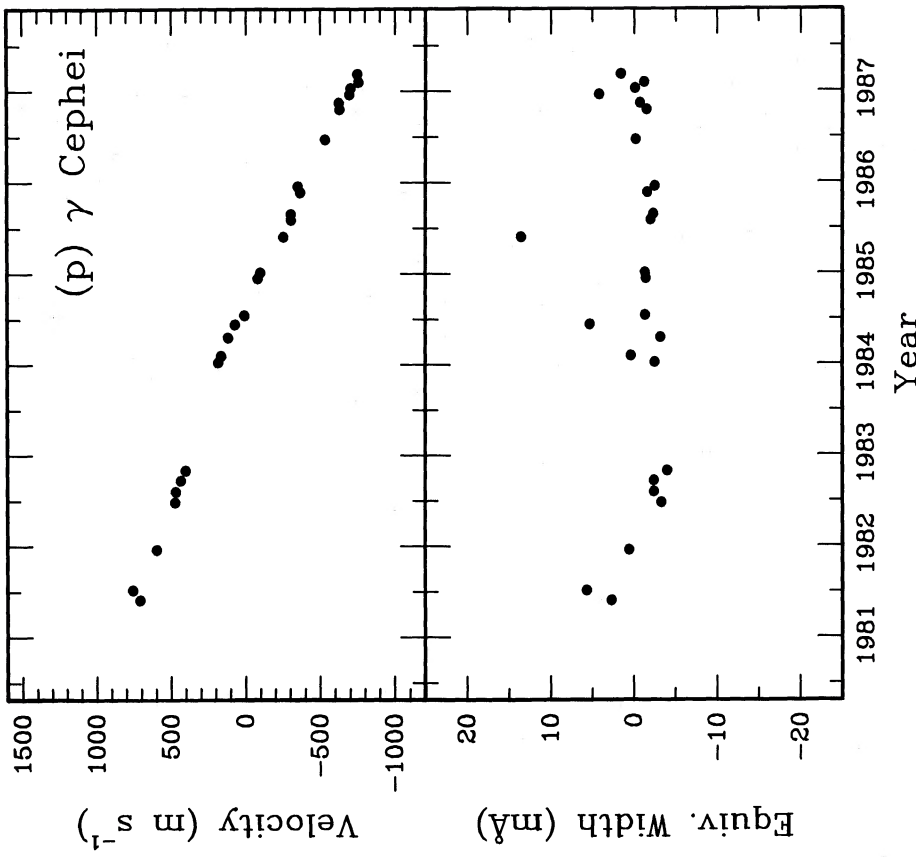


FIG. 2p

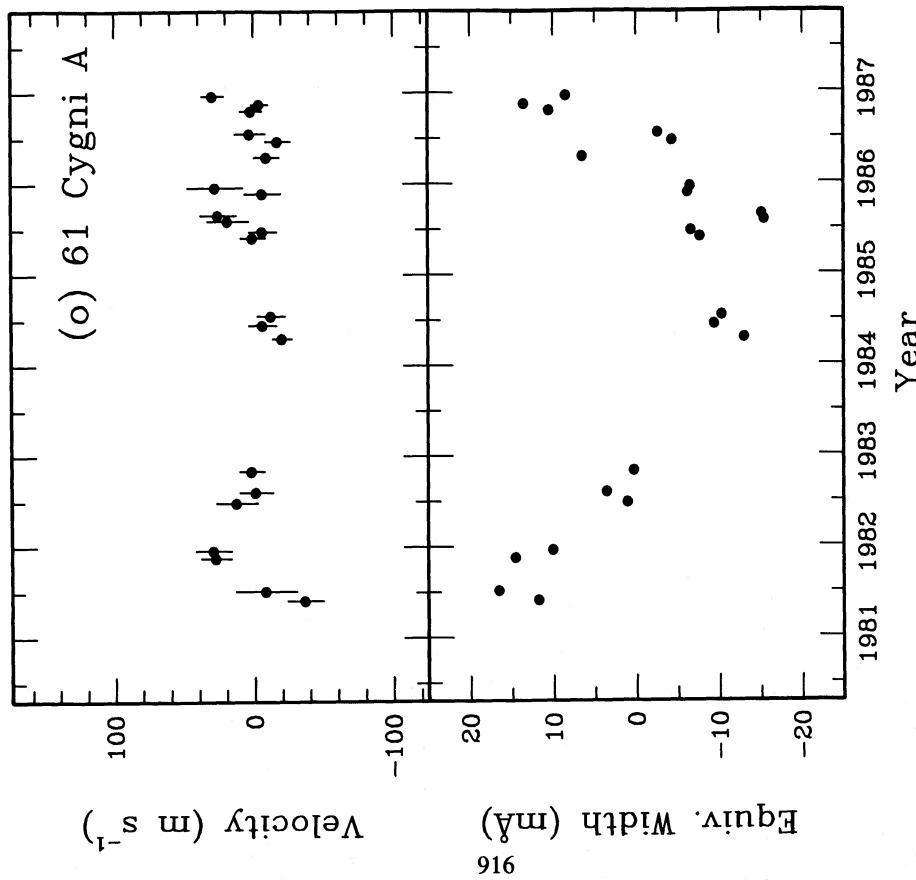


FIG. 2o

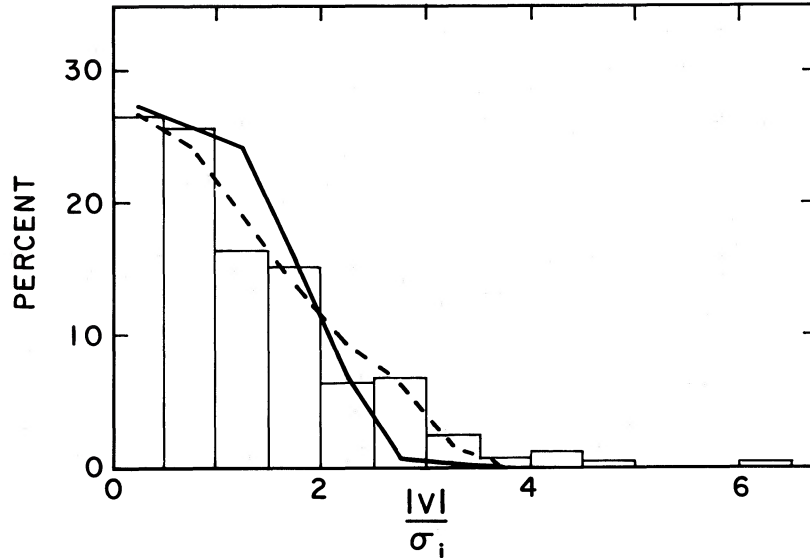


FIG. 3.—Histogram of velocities divided by internal errors for all stars except χ^1 Ori A and γ Cep. The curves show the distributions from simulated velocity data with no trend imposed (*solid*), and with a slope of $4 \text{ m s}^{-1} \text{ yr}^{-1}$ imposed (*dashed*).

tions, χ^1 Ori A (Fig. 2*d*) and γ Cep (Fig. 2*p*). The star χ^1 Ori A is varying under the influence of a stellar companion, and is discussed further below (§ IIIc). The star γ Cep was not previously suspected as a binary, but clearly the large variation observed over the past 6 years could well be due to a stellar companion. That is not the whole story for this star, however. The trend of decreasing velocity shown in Figure 2*p* is not smooth, but shows significant “bumps.” To illustrate this we have subtracted a second-order fit to the relative velocities, and the resulting residuals are shown in Figure 5. (The second-order fit was $V = -1.060 \times 10^{-4} \text{BJD}^2 + 0.5421 \text{BJD} + 514.0$, where $\text{BJD} = \text{barycentric Julian date} - 2,440,000$.) These velocity residuals show a periodic variation, with a semi-amplitude of about 25 m s^{-1} , and a period of about 2.7 yr. Since the 18.4 m

s^{-1} rms variation of these velocity residuals is larger than the external error for any other star, (see Table 3), and since our observations cover a full two periods of this variation, we classify γ Cep as a “probable” low-amplitude variable.

b) Are the Velocity Variations Due to Companions?

The low-level, long-term velocity variations that we have found in seven stars could, in principle, be due to something other than center-of-mass motion of the stars. However, it is unlikely that they are due to very long period stellar oscillations, since a simple radial variation at $\sim 10 \text{ m s}^{-1}$ over ~ 5 years would result in a doubling of the stellar radius. Similarly, starspots plus stellar rotation cannot produce the long-term trends, since spots would introduce a velocity modulation on

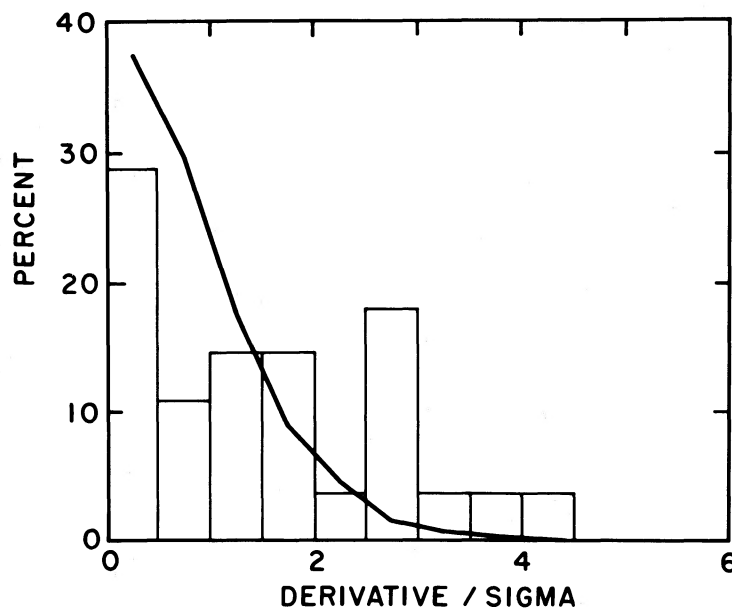


FIG. 4.—Histogram of observed $|S|/\sigma_s$ and $|C|/\sigma_c$ values from velocity curves of 14 stars. Continuous line shows the expected distribution from Monte Carlo simulations of 2000 data sets, if no trends in velocity are present.

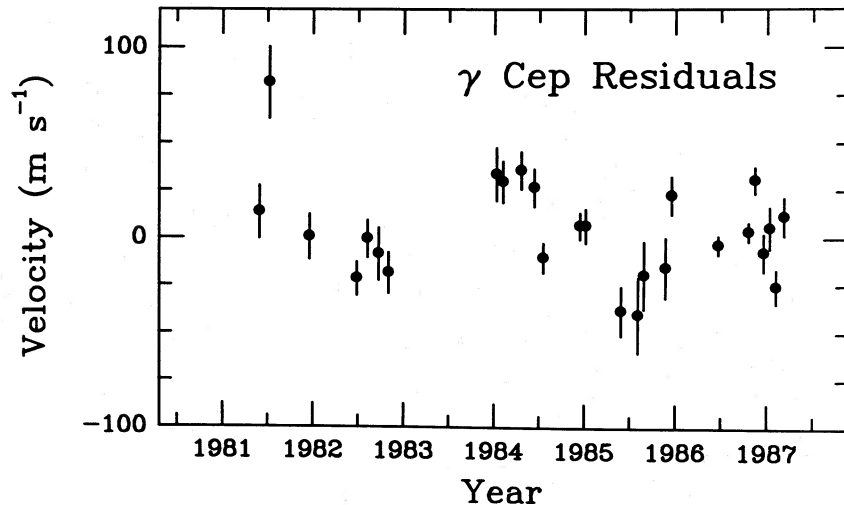


FIG. 5.—Velocity residuals for γ Cep after subtraction of a second order fit to the original velocities

the time scale of the stellar rotation period, which is less than ~ 1.5 months for solar-type stars (Vaughan *et al.* 1981; Baliunas *et al.* 1983).

A serious possibility, however, is that variations in convective granulation patterns on the time scale of stellar activity cycles could introduce apparent velocity variations, as suggested by Dravins (1985). Granulation patterns cause the line profile asymmetries observed in solar-type stars (e.g., Dravins, Lindegren, and Nordlund 1981; Dravins 1982; Gray and Toner 1985). It has been suggested that stellar activity cycles could modulate the granulation, perhaps through the influence of magnetic fields, affecting either the granule velocities or filling factors, or both. This could in turn cause variations of the line profiles on the time scale of the stellar activity cycle, leading to *apparent* velocity variations of perhaps a few times 10 m s^{-1} .

However, as suggested by Dravins (1985), such variations would presumably show a correlation with chromospheric activity indicators. Wilson (1978) has shown that the classic indicator of activity, the Ca II H- and K-line reversals, shows the effects of starspot cycles in solar-like stars. Fortunately, in our spectral region there is a line of Ca II, the infrared triplet line at 8662 \AA (see Fig. 1). This line does not show an emission reversal, but the core still shows the effects of filling-in by emission (Cayrel *et al.* 1983). In each of our spectra we have measured a relative equivalent width (arbitrary zero-point) of the central 1 \AA of the Ca II line. These values are given in column (6) of Table 1, and are plotted versus time for each star in Figure 2. The estimated uncertainty in the equivalent widths is typically 1 m\AA .

The coefficient of correlation between the velocities and Ca II equivalent widths, $r(V, \Delta EW)$, is shown in column (8) of Table 3. Taken individually, one might conclude that there are some possibly real correlations present (for example, ι Per and 36 UMa A). However, if there were a causal connection between the velocity and Ca II variations, predominantly positive or negative correlation coefficients would be anticipated. This is not observed; the average correlation coefficient is $+0.03$. We note that an occasional *apparent* correlation or anticorrelation would be expected if there are velocity variations due to low-mass companions on time scales similar to the cyclic variations in the Ca II line (which, incidentally, is the case

for the Sun). We conclude, therefore, that activity cycles do not affect radial velocities at the $\sim 10 \text{ m s}^{-1}$ level. In the absence of any other plausible origin for the velocity variations, we propose that they represent center-of-mass motion due to companions.

c) Notes on Individual Stars

In the following discussion, for stars which are close visual binaries, we have converted the astrometrically determined orbits to relative radial velocities using the prescription of van den Bos (1962). Parallaxes and V magnitudes have been taken from the *Bright Star Catalogue* (Hoffleit 1982), and where necessary these have been used to derive masses for dwarfs using an assumed mass-luminosity relation

$$\log M/M_{\odot} = -0.065M_V + 0.314 \quad (1)$$

a) HR 509 (τ Cet).—No astrometric perturbation found by Lippincott and Worth (1980) from 37 years of data. Ca II $\lambda 8662$ shows no evidence of variation, similar to the HK data of Wilson (1978). Campbell and Walker (1985) derived preliminary relative velocities for this star, which differ from the present results for the same data because of the more sophisticated reduction procedures currently employed.

b) HR 937 (ι Per).—No astrometric perturbation found by Lippincott and Worth (1980) from 63 years of data. We do not confirm the suspected velocity variability (Hoffleit 1982).

c) HR 1084 (ϵ Eri).—Probable variable. Van de Kamp (1974) proposed that there is a 25 year period perturbation with 0.019 semimajor axis, but our relative velocities are not consistent with this orbit. Heintz (1978) believes the orbit is spurious, since the nearby star δ Eri shows a similar perturbation. The single speckle interferometric detection of a companion by Blazit *et al.* (1977) has not been confirmed in 15 subsequent observations by McAlister (1986), nor by infrared speckle interferometry by McCarthy (1987). Noyes *et al.* (1984) found evidence of p -mode oscillations of about 10 minutes period. To minimize the effect of such oscillations on our velocities, our exposure times since 1984 have been a multiple of 10 minutes. *IRAS* data show a significant far-infrared excess (Aumann 1985).

d) HR 1325 (σ^2 Eri A).—No astrometric perturbation found by Heintz (1974) from 58 years of data. We do not confirm the

suspected velocity variability (Hoffleit 1982). Ca II $\lambda 8662$ shows clear evidence of cyclic behavior (Fig. 2*d*).

e) HR 2047 (χ^1 Ori A).—Velocities predicted from the astrometric orbit of Lippincott and Worth (1978), assuming B has negligible luminosity, are plotted along with our velocity data in Figure 2*e*. The agreement is satisfactory, considering the small astrometric amplitude. The eccentricity derived by Lippincott and Worth, 0.6, is obviously too large; a value around 0.35 is probably appropriate. We find no evidence for a late-type secondary spectrum from two of our spectra near velocity maximum and minimum (each of signal-to-noise ratio about 1500), and conclude that the magnitude difference in the *I*-band must be greater than 6.5 mag. This is nevertheless consistent with the speckle interferometric detection of χ^1 Ori B at 2.2 μm by McCarthy (1986). A secondary mass of 0.17 M_\odot (Lippincott and Worth 1978) is implied. We have not tested for a third body perturbation in our velocity data.

f) HR 4112 (36 UMa A).—Possible variable. Lippincott (1983) proposed that there is a close unseen companion to A. However, from her orbit, assuming this companion has negligible luminosity (note the nondetection by McCarthy [1986]), we predict an acceleration at 1984.0 of $|dV/dt| = 137 \text{ m s}^{-1} \text{ yr}^{-1}$. Since the observed acceleration is only $-4.7 \text{ m s}^{-1} \text{ yr}^{-1}$, we conclude that the suggested astrometric companion is spurious.

g) HR 4540 (β Vir).—Possible variable. Status of astrometric perturbations is unknown.

h) HR 4983 (β Com).—No astrometric perturbation found by Heintz (1986) from 53 years of data. We do not confirm the suspected velocity variability (Hoffleit 1982).

i) HR 5019 (61 Vir).—Possible variable. Status of astrometric perturbations is unknown.

j) HR 5544 (ξ Boo A).—From the astrometric orbit of Wielen (1962) and the mass ratio of Hershey (1977), we predict that the acceleration of A due to B should be $+12.3 \pm 0.8 \text{ m s}^{-1}$ at 1984.0. The observed acceleration is only $+5.0 \pm 1.7 \text{ m s}^{-1} \text{ yr}^{-1}$, which differs from the prediction at the 3.9 σ level (where σ includes the errors in both the predicted and observed accelerations). Uncertainties in the visual binary elements and mass ratio are too small to explain the discrepancy. We therefore classify this star as a possible variable due to a third body. Strand (1943*a*) and Walbaum and Duvent (1983) have suggested from astrometric observations that there is a third body in the system, but it cannot be a companion to A, since the proposed astrometric perturbations would imply a much larger velocity variation than we observe.

k) HR 7462 (σ Dra).—No periodic astrometric perturbation found by Heintz (1987) from 50 years of data. We do not confirm the suspected velocity variability (Hoffleit 1982).

l) HR 7602 (β Aql A).—Possible variable. Component B is dm3 at 13", with unknown orbit. It is therefore possible that the observed acceleration could be due to B alone.

m) HR 7948 (γ^2 Del).—Hopmann (1973) has given a provisional orbit for the $\gamma^1 - \gamma^2$ Delphini system ($P = 3249 \text{ yr}$). This yields an expected acceleration of $|dV/dt| = 0.6 \text{ m s}^{-1} \text{ yr}^{-1}$ at 1984.0. We do not confirm the suspected velocity variability (Hoffleit 1982).

n) HR 7957 (η Cep).—No astrometric perturbation found by Heintz (1986) from 45 years of data.

o) HR 8085 (61 Cyg A).—From the astrometric orbit of Josties (1983) we predict that the acceleration of A due to B should be $-3.7 \text{ m s}^{-1} \text{ yr}^{-1}$ at 1984.0. The sign of this acceleration was determined from a single spectrum of 61 Cyg B

obtained with HF on 1986.4723, which gave a velocity difference between the components $V_B - V_A = +1169 \pm 118 \text{ m s}^{-1}$. (The relatively large error is the result of differences in the spectra of A and B.) Using a parallax of 0".294, the predicted difference is 1261 m s^{-1} , which is in satisfactory agreement. A low-mass companion to either A or B was first suspected by Strand (1943*b*), while Deich (1978) identified low-level astrometric perturbations of 6 and 12 year periods. Our velocity data imply that if these perturbations are real, they must be in the B component. Heintz (1978) and Josties (1983) doubt the reality of these perturbations, while McAlister *et al.* (1987) and McCarthy (1987) saw no evidence of a companion to either A or B from speckle interferometry. Wilson's (1978) HK data for 61 Cyg A suggests a 7 year activity cycle. We would predict from Wilson's data a minimum around 1984, which is confirmed from our Ca II $\lambda 8662$ equivalent width measures (Fig. 2*o*).

p) HR 8974 (γ Cep).—Probable third body variation of 25 m s^{-1} amplitude, 2.7 yr period, superposed on a large velocity gradient. Status of astrometric perturbations is unknown.

IV. DISCUSSION

a) Limits to Companion Masses

For a companion of mass M_c (in Jupiter masses, M_J) in a circular orbit of period P (in years) and inclination i about a star of mass M_* (in solar masses), the derivatives of the radial velocity of the star will be

$$\frac{dV}{dt} = \frac{2\pi A}{P} \sin\left(\frac{2\pi t}{P} + \phi\right), \quad (2)$$

and

$$\frac{d^2V}{dt^2} = \frac{4\pi^2 A}{P^2} \cos\left(\frac{2\pi t}{P} + \phi\right), \quad (3)$$

where

$$A = \frac{28.4 M_c \sin i}{P^{1/3} M_*^{2/3}} \text{ m s}^{-1}. \quad (4)$$

Combining these yields

$$\left(\frac{dV}{dt}\right)^2 + \left(\frac{P}{2\pi}\right)^2 \left(\frac{d^2V}{dt^2}\right)^2 = \left(\frac{2\pi A}{P}\right)^2, \quad (5)$$

which is independent of the unknown phase, ϕ . Upper limits to the derivatives can be obtained from the slopes and curvatures derived above; the 1 σ upper limits for these are simply $|dV/dt| \leq S_{\text{max}} = |S| + \sigma_s$, and $|d^2V/dt^2| \leq C_{\text{max}} = |C| + \sigma_c$. Solving for the companion mass we have

$$M_c \sin i \leq 5.59 \times 10^{-3} P^{4/3} M_*^{2/3} \left[S_{\text{max}}^2 + \left(\frac{PC_{\text{max}}}{2\pi}\right)^2 \right]^{1/2}. \quad (6)$$

This yields an upper limit line in the mass-period plane, and an example of this for τ Cet is shown in Figure 6. For periods less than 6 years we have taken for an upper limit to the amplitude $A \leq 1.414 \sigma_e$ to derive the upper limit line from equation (4).

An additional constraint on companion masses comes from astrometric observations. Again assuming circular orbits we have that

$$M_c \leq 1.05 \times 10^3 \frac{\alpha_L}{\pi_p} \left(\frac{M_*}{P}\right)^{2/3}, \quad (7)$$

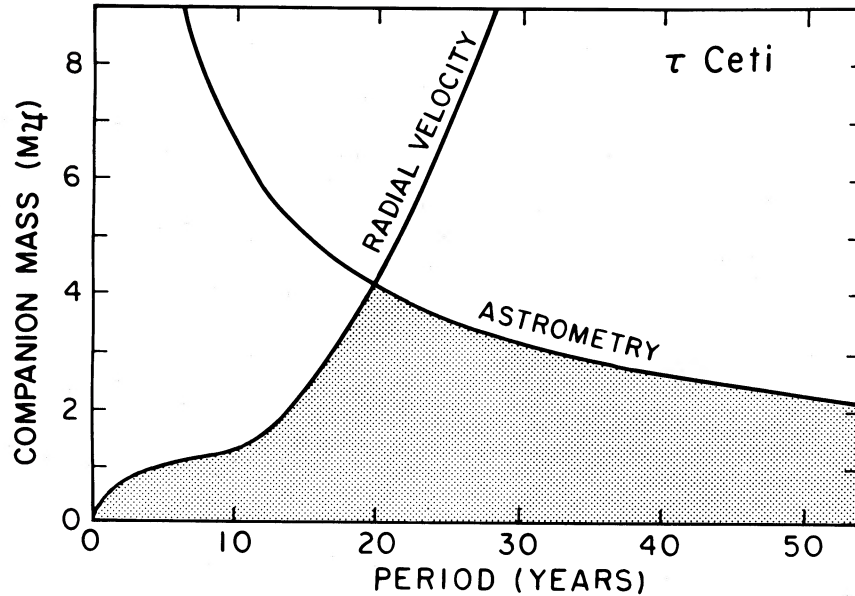


FIG. 6.—Companion mass-period diagram for τ Ceti. The radial velocity limit is from eq. (4) and eq. (6), while the astrometric limit is from eq. (7).

where π_p is the parallax, and α_L is the upper limit to astrometric perturbations. It is difficult to determine an appropriate value for α_L in all cases, because of the range in quality and types of data available. However, to our knowledge 13 of our 16 stars have been observed astrometrically, either to search for low-amplitude perturbations or to determine visual binary orbits, and none shows a convincing perturbation (due to third bodies in the visual binaries) larger than a few hundredths of an arcsecond. We therefore take as a representative 1σ upper limit $\alpha_L = 0''.01$.

Equation (7) yields the astrometric limit line in Figure 6. The intersection of the two lines in the mass-period plane gives a period-independent upper limit to the companion mass given by

$$M_c \sin^{1/3} i < 18.31 \left(\frac{\alpha_L M_*}{\pi_p} \right)^{2/3} \times \left[S_{\max}^2 + 2.91 \times 10^7 \left(\frac{\alpha_L}{\pi_p} \right)^3 \frac{(M_* C_{\max})^2}{(M_c \sin^{1/3} i)^3} \right]^{1/6}. \quad (8)$$

This expression yields the upper limits to the companion masses shown in column (9) of Table 3. The stellar masses were derived from equation (1) for dwarfs, from Hopmann (1973) for γ^2 Del, and from the evolutionary tracks of Vandenberg (1985) for β Aql, η Cep, and γ Cep. We stress that these upper limits are valid only for periods less than about 50 years, since this is the typical extent of the astrometric data.

The large range in these upper limits is primarily a result of the parallax dependence in equation (8). The median value of these upper limits is $8M_{21}$, or $9M_{21}$ if we allow for the average value of $\sin^{1/3} i$. We shall therefore say that $9M_{21}$ is the representative 1σ upper limit to companion masses for $P \leq 50$ yr.

For the possible or probable variables we have derived lower limits to the companion masses by taking half the observed velocity variation as a lower limit to the amplitude, and 12 years (twice the interval of our observations) as the lower limit to the period. These are given in column (9) of Table 3, and range from 0.9 to $1.6M_{21}$.

For γ Cep, the third body in the system has $M_c \sin i \sim 1.7M_{21}$. Since we have identified a period to the radial veloc-

ity variations, the lack of information on astrometric perturbations is not a concern in this case. This star therefore has the firmest evidence for a very low mass companion.

In summary, we find that of the 15 stars examined (χ^1 Ori A is not considered here), none shows evidence of a moderately close ($P \leq 50$ yr) companion of mass greater than roughly $10M_{21}$. Seven stars do show evidence of companions in the $1-9M_{21}$ range, assuming that these companions have orbital periods less than 50 years (which is certainly true for γ Cep).

b) The Companion Objects—Brown Dwarfs or Planets?

It is clear that none of our program stars has a close substellar-mass companion in the brown dwarf range of $\sim 10-80M_{21}$. This is consistent with many other recent surveys for brown dwarfs, which have so far failed to turn up a single confirmed candidate. The report by McCarthy, Probst, and Low (1985) of a brown dwarf companion to Van Biesbroeck 8 was apparently erroneous (Skrutskie, Forrest, and Shure 1987; Perrier and Mariotti 1987). Infrared searches for faint companions to red and white dwarfs in the field and open clusters by Probst and O'Connell (1982), Jameson, Sherrington, and Giles (1983), Zuckerman and Becklin (1987), and Kumar (1987) have turned up no substellar companions to brightness limits corresponding to about $30-40M_{21}$. Searches for isolated brown dwarfs by Boeshaar and Tyson (1985), Chester *et al.* (1986), and Boeshaar, Tyson, and Seitzer (1986) have failed to identify any candidates.

It can be argued that the mass limits set by the foregoing surveys depend on poorly understood cooling curves for brown dwarfs. This cannot be said for the survey of Marcy *et al.* (1986), in which they sought dynamical evidence of low-mass companions. They monitored 65 M dwarfs for low-amplitude velocity variations, and found none consistent with a brown dwarf down to a limit of about $10M_{21}$. (Marcy [1987] now believes that the companion to Gliese 623 is stellar.) All of this evidence suggests that brown dwarfs are rare, or perhaps non-existent, at least as companions to normal stars, and possibly also in the field.

If conventional brown dwarfs ($\sim 10-80M_{21}$) are so rare, at

least as companions to normal stars, how are we to classify the companion objects that we have found? For seven of 15 stars there is a "possible" or "probable" companion in the range $\sim 1\text{--}9M_{\oplus}$, assuming periods less than 50 years. Such a preponderance of very low mass companions, combined with the absence of conventional brown dwarfs, implies that there is a gap in the distribution of substellar mass objects. This suggests that the seven companions we have tentatively detected might be more closely related to planets than to brown dwarfs, and that these objects could represent the tip of the planetary mass spectrum. Additional information is required before a firm conclusion on the nature of these companions can be reached.

We are indebted to the staff of CFHT for their invaluable assistance with the HF cell observations, and to the Time Allo-

cation Committee of CFHT for their strong support of this long-term project. We are grateful to Harold McAlister and Don McCarthy for transmitting their unpublished results of speckle interferometric observations. For their advice and assistance we thank Bill van Altena, John Amor, Felix Aubke, Michael de Robertis, Murray Fletcher, George Gatewood, Bob Harrington, David Hartwick, Wulff Heintz, Gerhard Herzberg, Karl Kamper, Andy Lafontaine, Barbara Long, Geoff Marcy, Chris Morbey, Chris Pritchett, Randy Pyke, Dieter Schreiber, and Charles Worley. B. C. acknowledges the financial support of the National Research Council of Canada and the Canada Employment and Immigration Commission. The work of G. A. H. W. and S. Y. was supported in part by a grant from the Natural Sciences and Engineering Research Council to G. A. H. W.

REFERENCES

- Aumann, H. H. 1985, *Pub. A.S.P.*, **97**, 885.
 Baliunas, S. L., et al. 1983, *Ap. J.*, **275**, 752.
 Black, D. C. 1980, *Space Sci. Rev.*, **25**, 35.
 ———. 1986, in *Astrophysics of Brown Dwarfs*, ed. M. C. Kafatos, R. S. Harrington, and S. P. Maran (Cambridge: Cambridge University Press), p. 139.
 Blazit, A., Bonneau, D., Koechlin, L., and Labeyrie, A. 1977, *Ap. J. (Letters)*, **214**, L79.
 Boeshaar, P. C., and Tyson, J. A. 1985, *A.J.*, **90**, 817.
 Boeshaar, P. C., Tyson, J. A., and Seitzer, P. 1986, in *Astrophysics of Brown Dwarfs*, ed. M. C. Kafatos, R. S. Harrington, and S. P. Maran (Cambridge: Cambridge University Press), p. 76.
 Bracewell, R. N., and MacPhie, R. H. 1979, *Icarus*, **38**, 136.
 Campbell, B. 1983, *Pub. A.S.P.*, **95**, 577.
 Campbell, B., and Walker, G. A. H. 1979, *Pub. A.S.P.*, **91**, 540.
 ———. 1985, in *IAU Colloquium 88, Stellar Radial Velocities*, ed. A. G. D. Philip and D. W. Latham (Schenectady: L. Davis Press), p. 5.
 Campbell, B., Walker, G. A. H., Johnson, R., Lester, T., Yang, S., and Auman, J. 1981, *Proc. S.P.I.E.*, **290**, 215.
 Campbell, B., Walker, G. A. H., Pritchett, C., and Long, B. 1986, in *Astrophysics of Brown Dwarfs*, ed. M. C. Kafatos, R. S. Harrington, and S. P. Maran (Cambridge: Cambridge University Press), p. 37.
 Cayrel, R., Cayrel de Strobel, G., Campbell, B., Mein, N., Mein, P., and Dumont, S. 1983, *Astr. Ap.*, **123**, 89.
 Chester, T. J., Fullmer, L. D., Beichman, C. A., Gillet, F. C., Low, F. J., and Neugebauer, G. 1986, *Bull. A.A.S.*, **18**, 961.
 D'Antona, F., and Mazzitelli, I. 1985, *Ap. J.*, **296**, 502.
 Deich, A. N. 1978, *Pis'ma Astr. Zh.*, **4**, 95 (English trans. in *Soviet Astr. Letters*, **4**, 50).
 Dravins, D. 1982, *Ann. Rev. Astr. Ap.*, **20**, 61.
 ———. 1985, in *IAU Colloquium 88, Stellar Radial Velocities*, ed. A. G. D. Philip and D. W. Latham (Schenectady: L. Davis Press), p. 311.
 Dravins, D., Lindegren, L., and Nordlund, Å. 1981, *Astr. Ap.*, **96**, 345.
 Fahlman, G. G., and Glaspey, J. W. 1973, in *Astronomical Observations with Television-type Sensors*, ed. J. W. Glaspey and G. A. H. Walker (Vancouver: University of British Columbia), p. 347.
 Gray, D. F., and Toner, C. G. 1985, *Pub. A.S.P.*, **97**, 543.
 Griffin, R., and Griffin, R. 1973, *M.N.R.A.S.*, **162**, 243.
 Heintz, W. D. 1974, *A.J.*, **79**, 819.
 ———. 1978, *Ap. J.*, **220**, 931.
 ———. 1986, *A.J.*, **92**, 446.
 ———. 1987, private communication.
 Hershey, J. L. 1977, *A.J.*, **82**, 179.
 Herzberg, G. 1978, private communication.
 Hoffleit, D. 1982, *The Bright Star Catalogue* (New Haven: Yale University Observatory).
 Hopmann, J. 1973, *Astr. Mitt. Wein*, No. 13.
 Jameson, R. F., Sherrington, M. R., and Giles, A. B. 1983, *M.N.R.A.S.*, **205**, 39p.
 Josties, F. J. 1983, in *IAU Colloquium 62, Current Techniques in Double and Multiple Star Research*, ed. R. S. Harrington and O. G. Franz (Flagstaff: Lowell Observatory), p. 16.
 Kumar, C. K. 1987, preprint.
 Lippincott, S. L. 1983, *Pub. A.S.P.*, **95**, 775.
 Lippincott, S. L., and Worth, M. D. 1978, *Pub. A.S.P.*, **90**, 330.
 ———. 1980, *A.J.*, **85**, 171.
 Marcy, G. W. 1987, private communication.
 Marcy, G. W., Lindsay, V., Bergengren, J., and Moore, D. 1986, in *Astrophysics of Brown Dwarfs*, ed. M. C. Kafatos, R. S. Harrington, and S. P. Maran (Cambridge: Cambridge University Press), p. 50.
 McAlister, H. A. 1986, private communication.
 McAlister, H. A., Hartkopf, W. I., Hutter, D. J., Shara, M. M., and Franz, O. G. 1987, *A.J.*, **93**, 183.
 McCarthy, D. W., Jr. 1986, in *Astrophysics of Brown Dwarfs*, ed. M. C. Kafatos, R. S. Harrington, and S. P. Maran (Cambridge: Cambridge University Press), p. 9.
 ———. 1987, private communication.
 McCarthy, D. W., Jr., Probst, R. G., and Low, F. J. 1985, *Ap. J. (Letters)*, **290**, L9.
 Noyes, R. W., Baliunas, S. L., Belserene, E., Duncan, D. K., Horne, J., and Widrow, L. 1984, *Ap. J. (Letters)*, **285**, L23.
 Perrier, C., and Mariotti, J.-M. 1987, *Ap. J. (Letters)*, **312**, L27.
 Pritchett, C. J., Mochnacki, S., and Yang, S. 1982, *Pub. A.S.P.*, **94**, 733.
 Probst, R. G. 1983a, *Ap. J.*, **274**, 237.
 ———. 1983b, *Ap. J. Suppl.*, **53**, 335.
 Probst, R. G., and O'Connell, R. W. 1982, *Ap. J. (Letters)*, **252**, L69.
 Shipman, H. L. 1986, in *Astrophysics of Brown Dwarfs*, ed. M. C. Kafatos, R. S. Harrington, and S. P. Maran (Cambridge: Cambridge University Press), p. 71.
 Skrutskie, M. F., Forrest, W. J., and Shure, M. A. 1986, in *Astrophysics of Brown Dwarfs*, ed. M. C. Kafatos, R. S. Harrington, and S. P. Maran (Cambridge: Cambridge University Press), p. 82.
 ———. 1987, *Ap. J. (Letters)*, **312**, L55.
 Strand, K. Aa. 1943a, *Pub. A.S.P.*, **55**, 28.
 ———. 1943b, *Pub. A.S.P.*, **55**, 29.
 Stumpff, P. 1980, *Astr. Ap. Suppl.*, **41**, 1.
 van de Kamp, P. 1974, *A.J.*, **79**, 491.
 Vandenberg, D. A. 1985, *Ap. J. Suppl.*, **58**, 711.
 van den Bos, W. H. 1962, in *Astronomical Techniques*, ed. W. A. Hiltner (Chicago: University of Chicago Press), p. 537.
 Vaughan, A. H., Baliunas, S. L., Middelkoop, F., Hartmann, L. W., Mihalas, D., Noyes, R. W., and Preston, G. W. 1981, *Ap. J.*, **250**, 276.
 Walbaum, M., and Duvent, J.-L. 1983, *L'Astronomie*, **97**, 277.
 Walker, G. A. H., Johnson, R., and Yang, S. 1985, *Adv. Electronics Electron Phys.*, **64A**, 213.
 Wielen, R. 1962, *A.J.*, **67**, 599.
 Wilson, O. C. 1978, *Ap. J.*, **226**, 379.
 Zuckerman, B., and Becklin, E. E. 1987, *Ap. J. (Letters)*, **319**, L99.

BRUCE CAMPBELL: 4537 Rithetwood Place, Victoria, BC V8X 4J9, Canada

G. A. H. WALKER and S. YANG: Department of Geophysics and Astronomy, University of British Columbia, 2219 Main Mall, Vancouver, BC V6T 1W5, Canada